(This is a sample cover image for this issue. The actual cover is not yet available at this time.)

Transportation Research Part B 46 (2012) 1000–1022

Contents lists available at SciVerse ScienceDirect

Transportation Research Part B

journal homepage: www.elsevier.com/locate/trb

A kinematic wave theory of multi-commodity network traffic flow

Wen-Long Jin *

Department of Civil and Environmental Engineering, California Institute for Telecommunications and Information Technology, Institute of Transportation Studies, 4000 Anteater Instruction and Research Bldg., University of California, Irvine, CA 92697-3600, United States

ARTICLE INFO

Article history:
Received 27 October 2010
Received in revised form 23 February 2012
Accepted 23 February 2012

Keywords:
Lighthill–Whitham–Richards model
Multi-commodity Cell Transmission Model
Fair merging
First-in-first-out diverging
Riemann problem
Entropy conditions

ABSTRACT

A systematic understanding of traffic dynamics on road networks is crucial for many transportation studies and can help to develop more efficient ramp metering, evacuation, signal control, and other management and control strategies. In this study, we present a theory of multi-commodity network traffic flow based on the Lighthill–Whitham–Richards (LWR) model. In particular, we attempt to analyze kinematic waves of the Riemann problem for a general junction with multiple upstream and downstream links. In this theory, kinematic waves on a link can be determined by its initial condition and prevailing stationary state. In addition to a stationary state, a flimsy interior state can develop next to the junction on a link. In order to pick out unique, physical solutions, we introduce two types of entropy conditions in supply-demand space such that (i) speeds of kinematic waves should be negative on upstream links and positive on downstream links, and (ii) fair merging and First-In-First-Out diverging rules are used to prescribe fluxes from interior states. We prove that, for given initial upstream demands, turning proportions, and downstream supplies, there exists a unique critical demand level satisfying the entropy conditions. It follows that stationary states and kinematic waves on all links exist and are unique, since they are uniquely determined by the critical demand level. For a simple model of urban or freeway intersections with four upstream and four downstream links, we demonstrate that theoretical solutions are consistent with numerical ones from a multi-commodity Cell Transmission Model. In a sense, the proposed theory can be considered as the continuous version of the multi-commodity Cell Transmission Model with fair merging and First-In-First-Out diverging rules. Finally we discuss future research topics along this line.

1. Introduction

Traffic dynamics on a road network are determined by its travel demands, road topology, and drivers' behaviors (Newell, 1980). Once travel demands are given for all origin–destination pairs and related routes, various signalized and unsignalized intersections are the most important bottlenecks, which regulate the formation, propagation, and dissipation of traffic congestion. Since traffic flow theory is a cornerstone for all studies of transportation networks, a solid understanding of traffic dynamics around network intersections is crucial for transportation engineering and science: practically, it is helpful for developing more efficient ramp metering (Papageorgiou and Kotsialos, 2002), evacuation (Sheffi et al., 1982), signal control, and other management and control strategies; theoretically, it can yield better network loading models for transportation planning and management (Wu et al., 1998). A systematic understanding of traffic dynamics in a road network could also be useful for studies on blood flow in an arterial network (Formaggia et al., 2003; Ruan et al., 2003), fluid flow in a general

* Tel.: +1 949 824 1672; fax: +1 949 824 8385.
E-mail address: wjin@uci.edu

0191-2615/$ - see front matter © 2012 Elsevier Ltd. All rights reserved.
http://dx.doi.org/10.1016/j.trb.2012.02.009

vascular network (Sherwin et al., 2003), flow of goods along supply chains (Gottlich et al., 2005), and information flow on communication networks (D'apice et al., 2007; D'Apice et al., 2008).

For traffic flow on a road link, the first-order Lighthill–Whitham–Richards (LWR) model (Lighthill and Whitham, 1955; Richards, 1956) has been widely used to describe its dynamics as combinations of shock and rarefaction waves. In the LWR model, a fundamental diagram, which can be determined by as few as two parameters in the Greenshields model (Greenshields, 1935), is used to capture basic interactions among drivers and roads. Some nonequilibrium effects such as instability and hysteresis have been analyzed with higher-order kinematic wave models (Payne, 1971; Whitham, 1974). In transportation planning studies, link performance functions have been applied to analyze network traffic flow (Wardrop, 1952; Dafermos and Sparrow, 1969; Merchant and Nemhauser, 1978). However, these models over-simplify traffic dynamics without describing traffic waves or bottlenecks correctly (Daganzo, 1995a). In traffic operation studies, numerous simulators have been developed based on microscopic models of individual vehicles' behaviors (e.g. Gazis et al., 1961; Gipps, 1986; Hidas, 2002; Hidas, 2005). But simulation-based studies do not provide systematic approaches to analyzing traffic dynamics at the network level. In other efforts, the LWR model or higher-order models were extended to include source terms for on-ramp or off-ramp flows (Liu et al., 1996; Herty and Klar, 2003). This approach is simple but omits interactions among traffic streams by assuming that on-ramp or off-ramp flows are not impacted by mainline freeway traffic.

Traffic dynamics on a road network can be quite complicated due to interactions among merging, diverging, and other bottlenecks (Daganzo, 1996; Jin, 2009). In order to obtain a systematic understanding of traffic dynamics caused by network bottlenecks, there have been two important trends of research within the framework of kinematic wave models since the middle of 1990s. In one line, attempts have been made to develop unified theories to analyze kinematic waves of network traffic flow. In (Holden and Risebro, 1995), traffic dynamics on each link are described by the LWR model, and additional entropy conditions are introduced to uniquely find traffic flows through a general junction with multiple upstream and downstream links and corresponding kinematic waves on all links. In this study, for Riemann problems with jump initial conditions, it is shown that each link will be prevailed by a stationary state, and the kinematic wave on the link can be determined by the LWR model with initial and stationary states as corresponding upstream and downstream conditions. Then two entropy conditions are employed to find such stationary states: (i) speeds of kinematic waves on upstream and downstream links have to be negative and positive, respectively; and (ii) link fluxes optimize an objective function in stationary densities. But this theory is for uni-modal traffic, since vehicles do not have predefined routes, and the second entropy condition is pragmatic and not explicitly related to physical merging and diverging rules. In (Coclite et al., 2005), kinematic wave solutions are analyzed when a turning proportion matrix is given, but this analysis is only valid when a junction has no more upstream links than downstream links. In (Garavello and Piccoli, 2005; Garavello and Piccoli, 2006a; Herty et al., 2006; Haut and Bastin, 2007; Herty et al., 2008), more extensions along this line have been proposed to incorporate higher-order models for link traffic flow. Similar to (Holden and Risebro, 1995), the employed entropy conditions usually lack physical meanings in these studies.

In the other line, Daganzo (1995b) and Lebacque (1996) extended the Godunov discrete form of the LWR model to compute traffic flows through merging, diverging, and general junctions. In these Cell Transmission Models (CTMs), so-called traffic demand and supply functions are introduced, and boundary fluxes through various types of junctions can be written as functions of upstream demands and downstream supplies. Within the framework of CTM, various merging and diverging rules can be incorporated (Daganzo, 1995b; Lebacque, 1996). For example, in (Jin and Zhang, 2004), a multi-commodity CTM was developed for simulating traffic dynamics on general road networks, in which traffic flows through junctions with multiple upstream and downstream links are calculated based on the First-In-First-Out (FIFO) diverging principle (Papageorgiou, 1990; Daganzo, 1995b) and the fair merging principle (Jin and Zhang, 2003b). Such diverging and merging rules have been verified by observations at the aggregate level (Muñoz and Daganzo, 2002; Lebacque, 2005; Ni and Leonard, 2005; Cassidy and Ahn, 2005; Bar-Gera and Ahn, 2010). CTM has been widely used as network loading models for solving dynamic traffic assignment and other problems (Buisson et al., 1996; Lo and Szeto, 2002; Bliemer, 2007; Durlin and Henn, 2008). However, CTM is in nature discrete simulation models and does not provide any analytical insights on congestion formation at a network intersection.

In this study, we attempt to present a new kinematic wave theory of multi-commodity network traffic flow, which extends the analytical framework of (Holden and Risebro, 1995) but incorporates physical merging and diverging rules used in CTM into the entropy conditions. Traditionally, for such a hyperbolic conservation law as the LWR model, an entropy condition is presented in terms of characteristic wave speeds (Lax, 1972): there exists a discontinuous shock wave if and only if the upstream characteristic speed is higher than the downstream one. As pointed out by (Ansorge, 1990), this entropy condition is physical on a road link: there exists a discontinuous shock wave if and only if the downstream traffic is more congested. Such entropy conditions have been extended for inhomogeneous LWR model (Jin and Zhang, 2003a). But for a network junction with multiple upstream and downstream links, there have been no simple entropy conditions in terms of characteristic waves. Instead, in this study, we extends the analytical framework of (Holden and Risebro, 1995) to solve kinematic waves arising from a network junction. (i) As observed in (Holden and Risebro, 1995), a stationary state prevails a link in Riemann solutions, and the kinematic wave on the link is determined by the LWR model with initial and stationary states as corresponding upstream and downstream conditions. (ii) Also as observed in (Holden and Risebro, 1995), kinematic waves determined by initial and stationary states have to possess correct signs: negative on upstream links, and positive on downstream links. (iii) But different from (Holden and Risebro, 1995), we introduce on each link a flimsy interior state next to the junction in the Riemann solutions. Such an interior state does not take any space in the continuous solution and is

therefore inconsequential in the weak solutions. Since the interior state should not impact the kinematic wave on the link, the kinematic wave determined by the stationary and interior state has to be suppressed by having an opposite sign as the kinematic wave on the link. But the interior state shows up in the cell next to the junction in the numerical solutions as observed for Burgers' equation (van Leer, 1984; Bultelle et al., 1998) and the inhomogeneous LWR model (Jin and Zhang, 2003a). (iv) Also different from (Holden and Risebro, 1995), we use fair merging and FIFO diverging rules in the multi-commodity CTM (Jin and Zhang, 2004) as an additional entropy condition to prescribe boundary fluxes from interior states. (v) In addition, we solve stationary states in supply-demand space, rather than in density-flux space. The choice of supply-demand space is quite natural and helps to simplify the analyses, since the merging and diverging rules are given in terms of upstream demands and downstream supplies.

The aforementioned analytical framework was first devised for solving the Riemann problem of inhomogeneous LWR model at a linear junction in (Jin et al., 2009). In (Jin, 2010c), traffic dynamics at merging junctions with two upstream links were discussed by incorporating fair, priority-based, and constant merging rules into the entropy conditions. In (Jin, 2010b), traffic dynamics at diverging junctions with two downstream links were discussed by incorporating FIFO and evacuation diverging rules into the entropy conditions. In this paper, we further study traffic dynamics at general junctions with multiple upstream and downstream links. Here we incorporate into the entropy conditions the junction model developed in (Jin and Zhang, 2004), which is based on fair merging and FIFO diverging rules. After formulating the entropy conditions in supply-demand space, we define a critical demand level, which can be used to separate upstream stationary states into strictly over-critical and under-critical ones. Then we show that the entropy conditions are equivalent to maximizing the critical demand level and prove that stationary states and, therefore, kinematic waves on all links exist and are unique under given initial conditions. In the sense of (Garavello and Piccoli, 2006b), here we attempt to construct a Riemann solver for general network junctions with fair merging and FIFO diverging rules. But different from (Holden and Risebro, 1995; Coclite et al., 2005), the new Riemann solver is consistent with the discrete multi-commodity CTM.

The rest of the paper is organized as follows. In Section 2, we introduce a continuous multi-commodity kinematic wave model of network traffic and define the corresponding Riemann problem. In Section 3, we discuss entropy conditions, including feasible solutions of stationary and interior states, and the fair merging and FIFO diverging rules in supply-demand space. In Section 4, we define the critical demand level and prove that solutions to the Riemann problem exist and are unique. In Section 5, we numerically demonstrate that analytical solutions of traffic dynamics at a general intersection are consistent with those of CTM. In Section 6, we discuss future research directions.

2. A kinematic wave model of multi-commodity network traffic flow and the Riemann problem

In a general road network, e.g., the Braess network shown in Fig. 1, we denote the set of links by $\mathscr{A}$, the set of junctions by $\mathscr{J}$, and the set of paths by $\mathscr{P}$. When studying traffic dynamics, we assume that all time-dependent path demands are given from observations or through transportation planning studies. That is, we do not consider drivers' choice behaviors in modes, departure times, or routes.

2.1. A kinematic wave model of multi-commodity network traffic flow

In this study, we assume that all vehicles have pre-defined paths. As in (Jin and Zhang, 2004), vehicles using the same path belong to one commodity. For commodity $p \in \mathscr{P}$, we denote density, speed, and flow-rate by $\rho_p(x_p, t)$, $v_p(x_p, t)$, and $q_p(x_p, t) = \rho_p(x_p, t)v_p(x_p, t)$, respectively. Here x_p is the distance coordinate for commodity p. For link $a \in \mathscr{A}$, we denote density, speed, and flow-rate by $\rho_a(x_a, t)$, $v_a(x_a, t)$, and $q_a(x_a, t) = \rho_a(x_a, t)v_a(x_a, t)$, respectively. Here x_a is the distance coordinate for link a. Then we have

$$\rho_a(x_a, t) = \sum_p \delta_{p,a}\rho_p(x_a, t),$$

$$q_a(x_a, t) = \sum_p \delta_{p,a}q_p(x_a, t),$$

where $\delta_{p,a}$ is the commodity-link incidence function, equal to 1 when path p uses link a and 0 otherwise.

For link a, we have a traffic conservation equation:

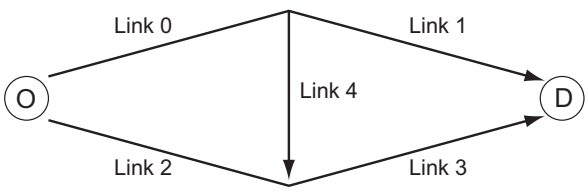

Fig. 1. The Braess network (Braess et al., 2005).

$$\frac{\partial}{\partial t}\rho_a(x_a,t)+\frac{\partial}{\partial x_a}q_a(x_a,t)=0. \tag{1}$$

Observations and car-following theories suggest that in steady states there exist a fundamental diagram (Greenshields, 1935; Del Castillo and Benitez, 1995) such that

$$q_a=Q(x_a,\rho_a), \tag{2}$$

which can be considered as a macroscopic model of vehicles' driving, especially car-following, behaviors. Generally a fundamental diagram is unimodal in $\rho_a \leqslant \rho_{a,j}$, where $\rho_{a,j}$ is the jam density. Correspondingly, speed–density relation, $V_a(x_a, \rho_a) = Q(x_a, \rho_a)/\rho_a$, is non-increasing in ρ_a, and $v_{a,f}(x_a) = V_a(x_a, 0)$ is the free flow speed. In addition, capacity is defined by $C_a(x_a) = Q_a(x_a, \rho_{a,c}(x_a)) \geqslant Q_a(x_a, \rho_a)$ for any ρ_a, where $\rho_{a,c}(x_a)$ is the critical density. Traffic states with densities higher than $\rho_{a,c}(x_a)$ are congested or over-critical (OC), and those with lower densities are free flowing or under-critical (UC). Combining traffic conservation Eq. (1) and the fundamental diagram (2) we obtain the link-based LWR model (Lighthill and Whitham, 1955; Richards, 1956):

$$\frac{\partial}{\partial t}\rho_a+\frac{\partial}{\partial x_a}Q_a(x_a,\rho_a)=0. \tag{3}$$

According to the LWR model, traffic dynamics can be considered as combinations of shock and rarefaction waves, which correspond to the formation and dissipation of traffic congestion, respectively.

In real traffic, different types of vehicles can have different speeds at the same location (Zhang and Jin, 2002) or are allowed to use different groups of lanes (Daganzo, 1997; Daganzo, 2002). Both of these scenarios could lead to different fundamental diagrams. In this study, we assume that vehicles of different commodity share the same speed at the same location and time. Thus for any commodity p using link a

$$v_p(x_a,t)=V_a(x_a,\rho_a). \tag{4}$$

If we define a commodity proportion by

$$\xi_p(x_a,t)=\frac{\rho_p}{\rho_a}=\frac{q_p}{q_a},$$

then we have the following equation (Lebacque, 1996)

$$\frac{\partial}{\partial t}\xi_p+V_a(x_a,\rho_a)\frac{\partial}{\partial x_a}\xi_p=0, \tag{5}$$

which implies that commodity proportions always travel forward at vehicles' speeds. (3) and (5) constitute a link-based multi-commodity kinematic wave model of network vehicular traffic. Correspondingly, we can have the following path-based kinematic wave model for commodity p ($p = 1, \ldots, P$)

$$\frac{\partial}{\partial t}\rho_p(x_p,t)+\frac{\partial}{\partial x_p}\xi_{p,a}(x_a,t)Q(\rho_a(x_a,t))=0. \tag{6}$$

We note that link-based and path-based kinematic wave models of multi-commodity network traffic flow are equivalent to each other in terms of their weak solutions (Holden and Risebro, 1995). Hereafter we refer to (3) and (5) or (6) as the kinematic wave model of multi-commodity network traffic flow.

For the original LWR model (3), which is a hyperbolic conservation law, its weak solutions may not be unique, and an entropy condition has to be introduced to pick out unique, physical solutions (Lax, 1972). It was shown that such an entropy condition in terms of characteristic wave speeds is consistent with vehicles' acceleration/deceleration behaviors (Ansorge, 1990). Such entropy conditions can be derived but become quite complicated for an inhomogeneous road (Jin and Zhang, 2003a). Similarly, the kinematic wave theory of multi-commodity network traffic flow in (6) can have non-unique weak solutions. On each link, traditional entropy conditions can be applied, but additional entropy conditions are necessary for traffic dynamics arising from merging, diverging, or other types of junctions. In (Holden and Risebro, 1995; Coclite et al., 2005), entropy conditions for network junctions were introduced based on proper signs of kinematic waves on all links as well as optimization schemes to determine fluxes through various junctions. In this study, we extend this framework to solve the multi-commodity kinematic wave models (6) for general network junctions. But we incorporate physical merging and diverging rules used in the multi-commodity CTM developed by (Jin and Zhang, 2004) into our entropy conditions.

2.2. The Riemann problem

In this study, we introduce entropy conditions for solving traffic dynamics around a general network junction shown in Fig. 2, which has m upstream links and n downstream links. In this network, there are totally mn commodities, and commodity p that uses upstream link a and downstream link b can be denoted by $a \to b$. As we know, the LWR model on a link cannot be analytically solved under general initial and boundary conditions. But by solving the Riemann problem with jump initial conditions, one can understand the formation of shock and rarefaction waves and therefore the fundamental properties of

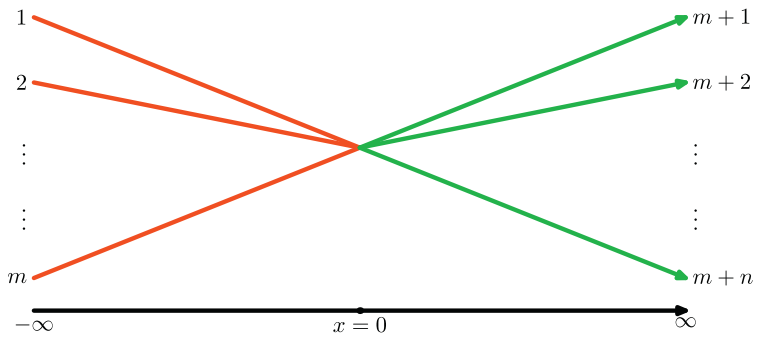

Fig. 2. A general network junction.

the LWR model. Similarly, here we attempt to solve the Riemann problem for the multi-commodity kinematic wave model. In this problem, all links are assumed to be homogeneous and infinitely long: for link $a = 1, \ldots, m+n$, its flow-density relation is $q_a = Q_a(\rho_a)$ with a critical density $\rho_{a,c}$ and capacity C_a. Note that different links can have different fundamental diagrams in our study. In addition, all links have constant initial conditions:

$$\rho_a(x_a, 0) = \rho_a, x_a \in (-\infty, 0), \quad a = 1, \ldots, m \tag{7a}$$

$$\rho_b(x_b, 0) = \rho_b, x_b \in (0, +\infty), \quad b = m+1, \ldots, m+n \tag{7b}$$

$$\xi_{a\to b}(x_a, 0) = \xi_{a\to b}, \quad a = 1, \ldots, m; \quad b = m+1, \ldots, m+n \tag{7c}$$

Note that at the junction $x_a = 0$ and $x_b = 0$ for all links, and therefore the network's initial conditions jump at the junction.

In particular, when $m = n = 1$, the junction in (2) is a linear junction, the multi-commodity kinematic wave model (3) and (5) is equivalent to the single-commodity LWR model, and the Riemann problem with initial conditions (7) is the same as the traditional Riemann problem. In this case, when both upstream and downstream links share the same fundamental diagram, then we have a homogeneous LWR model; otherwise, it becomes an inhomogeneous LWR model. Refer to (Lebacque, 1996) for seven types of kinematic wave solutions to the Riemann problem for the homogeneous LWR model. For the inhomogeneous LWR model, an additional entropy condition has to be introduced, and standing waves, in addition to shock and rarefaction waves, can appear in solutions to the Riemann problem (Jin and Zhang, 2003a). In (Holden and Risebro, 1995), the Riemann problem for a single-commodity kinematic wave model of general networks was studied without considering diverging proportions $\xi_{a\to b}$. In (Coclite et al., 2005), the Riemann problem for a multi-commodity kinematic wave model was studied for $m \leqslant n$. In both studies, all links are assumed to have the same fundamental diagram. In addition, in these and other studies along the line (Garavello and Piccoli, 2005; Garavello and Piccoli, 2006a; Herty et al., 2006; Haut and Bastin, 2007; Herty et al., 2008), pragmatic entropy conditions were used to pick out unique solutions, and it is not clear whether such solutions are consistent with drivers' merging and diverging behaviors or with observed data.

In (Jin et al., 2009), a new framework was proposed to solve the Riemann problem for an inhomogeneous link: the initial conditions were first mapped into supply-demand space, and then a boundary flux function used in CTM (Daganzo, 1995b; Lebacque, 1996), equal to the smaller one of upstream demand and downstream supply, was incorporated into entropy conditions. Within the same framework, in (Jin, 2010c), the Riemann problem when $m = 2$ and $n = 1$ was studied for fair, constant, and priority-based merging rules. In (Jin, 2010b), the Riemann problem when $m = 1$ and $n = 2$ was studied for FIFO and evacuation-based diverging rules. In this study, we attempt to further these studies by considering the Riemann problem for general network junctions. That is, we consider an arbitrary combination of m upstream links and n downstream links, and different links may have different fundamental diagrams with different numbers of lanes, speed limits, or grades. But we only consider entropy conditions based on fair merging and FIFO diverging rules developed in (Jin and Zhang, 2004), and other rules are subject to future discussions.

For link $a = 1, \ldots, m+n$ in Fig. 2, we define the following demand and supply functions (Engquist and Osher, 1980; Daganzo, 1995b; Lebacque, 1996)

$$D_a(\rho) = Q_a(\min\{\rho, \rho_{a,c}\}), \tag{8a}$$

$$S_a(\rho) = Q_a(\max\{\rho, \rho_{a,c}\}), \tag{8b}$$

where $D_a \leqslant C_a$ is non-decreasing in ρ, $S_a \leqslant C_a$ non-increasing, and

$$\max\{D_a, S_a\} = C_a.$$

In addition $D_a = S_a = C_a$ iff traffic is critical (C); $D_a < S_a = C_a$ iff traffic is strictly under-critical (SUC); $S_a < D_a = C_a$ iff traffic is strictly over-critical (SOC). Note that a UC state can be either C or SUC, and an OC state can be either C or SOC.

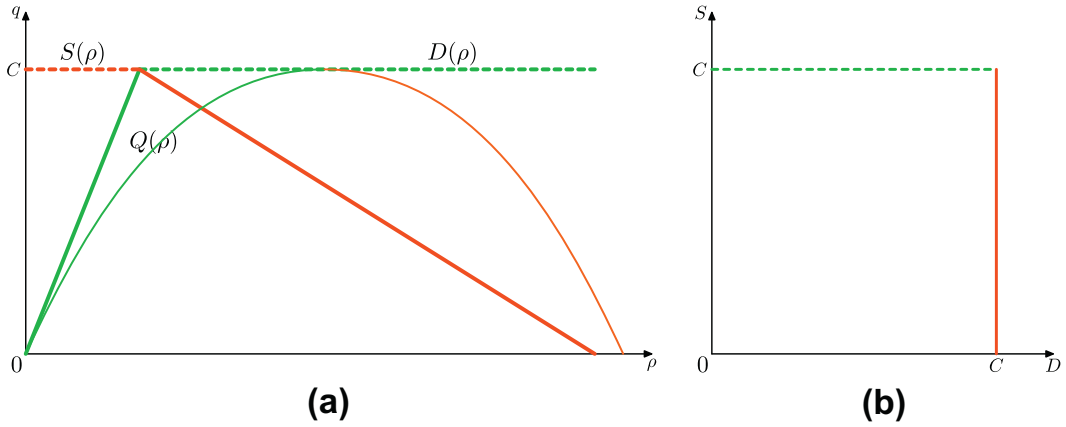

Fig. 3. Triangular and Greenshields fundamental diagrams and their corresponding supply-demand diagrams.

Different from traditional analyses in (Holden and Risebro, 1995; Coclite et al., 2005), where traffic conditions are represented by densities, here we represent a traffic state at (x, t) on link a by $U_a(x, t) = (D_a(x, t), S_a(x, t))$ in supply-demand space. We choose to work in supply-demand space since the fair merging and FIFO diverging rules were given in upstream demands and downstream supplies (Jin and Zhang, 2004). At $U_a(x, t)$, the corresponding flow-rate is

$$q_a(x,t) = \min\{D_a(x,t), S_a(x,t)\}.$$

In Fig. 3b, we draw a supply-demand diagram for the two fundamental diagrams in Fig. 3a. On the dashed branch of the supply-demand diagram, traffic is UC and $U = (D, C)$ with $D \leqslant C$; on the solid branch, traffic is OC and $U = (C, S)$ with $S \leqslant C$. Compared with the fundamental diagram of a road section, the supply-demand diagram only considers its capacity C and criticality, but not other detailed characteristics such as critical density, jam density, or shape of the fundamental diagram. That is, different fundamental diagrams can have the same demand-supply diagram, as long as they have the same capacity and are unimodal, and their critical densities, jam densities, or shapes are not relevant. However, given a demand-supply diagram and its corresponding fundamental diagram, the points are one-to-one mapped.

Therefore, traffic state $U_a = (D_a, S_a)$ is under-critical (UC), iff $S_a = C_a$, or equivalently $D_a \leqslant S_a$, or equivalently $U_a = (q_a, C_a)$; Traffic state $U_a = (D_a, S_a)$ is over-critical (OC), iff $D_a = C_a$, or equivalently $S_a \leqslant D_a$, or equivalently $U_a = (C_a, q_a)$. Since $D_a/S_a = -D_a(\rho)/S_a(\rho)$ is a strictly increasing function of ρ, $\rho_a(x, t)$ can be uniquely determined by $U_a(x, t)$. For example, we can introduce a function

$$\rho_a = K_a(D_a/S_a), \tag{9}$$

which can be considered as the inverse function of $q_a = Q_a(\rho_a)$. But note that densities cannot be determined from either demand or supply alone. That is, a complete traffic state has to be described by both demand and supply.

In supply-demand space, initial conditions in (7) can be re-written as

$$U_a(x_a, 0) = (D_a, S_a), x_a \in (-\infty, 0), \quad a = 1, \ldots, m \tag{10a}$$

$$U_b(x_b, 0) = (D_b, S_b), x_b \in (0, +\infty), \quad b = m+1, \ldots, m+n \tag{10b}$$

$$\xi_{a\to b}(x_a, 0) = \xi_{a\to b}, \quad a = 1, \ldots, m; \quad b = m+1, \ldots, m+n \tag{10c}$$

3. Entropy conditions in supply-demand space

In solutions to the Riemann problem of the kinematic wave model (6) with initial conditions in (10), a shock wave or a rarefaction wave could initiate on a link from the junction, and traffic states on all links become asymptotically stationary after a long time. Such stationary states can be considered as fixed points of discrete equations, CTM in this case (Bultelle et al., 1998). We denote the stationary states on upstream link $a(a = 1, \ldots, m)$ and downstream link $b(b = m + 1, \ldots, m + n)$ by U_a^* and U_b^*, respectively. Once we find stationary states in supply-demand space, we can calculate the corresponding stationary densities, ρ_a^* and ρ_b^*, from the fundamental diagrams. Then the kinematic wave on upstream link a is the solution of the corresponding LWR model with initial left and right conditions of ρ_a and ρ_a^*, respectively. That is, for upstream link a, we solve the following Riemann problem to obtain the corresponding kinematic wave:

$$\frac{\partial}{\partial t}\rho_a + \frac{\partial}{\partial x_a}Q_a(\rho_a) = 0, \tag{11}$$

with initial condition

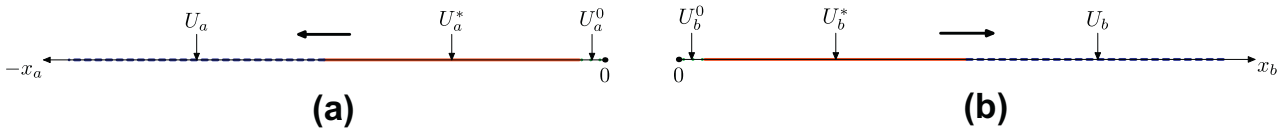

Fig. 4. Structure of Riemann solutions: (a) Upstream link a; (b) Downstream link b.

$$\rho_a(x_a, t=0) = \begin{cases} \rho_a, & x_a < 0, \\ \rho_a^*, & x_a > 0. \end{cases} \tag{12}$$

Similarly, the kinematic wave on downstream link b is the solution of the corresponding LWR model with initial left and right conditions of ρ_b^* and ρ_b, respectively. That is, for downstream link b, we solve the following Riemann problem to obtain the corresponding kinematic wave:

$$\frac{\partial}{\partial t}\rho_b + \frac{\partial}{\partial x_b} Q_b(\rho_b) = 0, \tag{13}$$

with initial condition

$$\rho_b(x_b, t=0) = \begin{cases} \rho_b^*, & x_b < 0, \\ \rho_b, & x_b > 0. \end{cases} \tag{14}$$

Solutions to the Riemann problem of such a hyperbolic conservation law have been discussed in (Lax, 1972) and in particular in (Lebacque, 1996).

In addition to stationary states, we further introduce interior states at the boundary of each link. Different from prevailing stationary states, such flimsy interior states only take infinitesimal space. On a link in discrete CTM, an interior state, if different from the corresponding stationary state, only shows up in the cell right next to the junction. We denote the interior states on links a and b by U_a^0 and U_b^0, respectively.[1]

Therefore, the structure of Riemann solutions on upstream and downstream links are shown in Fig. 4, where arrows illustrate the directions of possible kinematic waves.

In the Riemann solutions, boundary fluxes are time-independent, and we denote $q_{a\to b}$ as the flux from upstream link a to downstream link b for $t > 0$. Since the fluxes are determined by the stationary states, the out-flux of upstream link a is

$$q_a = q(U_a^*) = \min\{D_a^*, S_a^*\}, \tag{15a}$$

and the in-flux of downstream link b is

$$q_b = q(U_b^*) = \min\{D_b^*, S_b^*\}. \tag{15b}$$

In stationary states $\xi_{a\to b}^* = \xi_{a\to b}$ on upstream links since commodity proportions travel forward, according to (5). From traffic conservation, we have

$$q_{a\to b} = q_a \xi_{a\to b}^* = q_a \xi_{a\to b}, \tag{16a}$$

and

$$q_a = \sum_{b=m+1}^{m+n} q_{a\to b}, \quad q_b = \sum_{a=1}^{m} q_{a\to b}, \quad q = \sum_{a=1}^{m} q_a = \sum_{b=m+1}^{m+n} q_b \tag{16b}$$

3.1. Admissible stationary and interior states

As observed in (Holden and Risebro, 1995; Coclite et al., 2005) kinematic waves of (11) with initial conditions (12) cannot have positive speeds, and those of (13) with initial conditions (14) cannot have negative speeds. Feasible domains of stationary traffic densities were derived in terms of stationary densities in (Holden and Risebro, 1995). In contrast, we represent the feasible domains in supply-demand space. In addition, we also derive feasible domains of interior states. These admissible conditions constitute the first entropy conditions.

We have the following admissible conditions on stationary states.

Lemma 3.1 (*Admissible stationary states*). *For initial conditions in* (10), *stationary states are admissible if and only if*

$$U_a^* = (D_a, C_a) \text{ or } (C_a, S_a^*), \tag{17a}$$

[1] It can be shown that $\rho(x,t) = \begin{cases} \rho_L, & x < 0 \\ \rho_M, & x = 0 \\ \rho_R, & x > 0 \end{cases}$ is a solution to $\frac{\partial \rho}{\partial t} + \frac{\partial Q(\rho)}{\partial x} = 0$, if $\rho_L < \rho_M < \rho_R$ and $Q(\rho_L) = Q(\rho_R)$. That is, an interior state, ρ_M, can exist with a stationary shock wave in the LWR model. At a junction, it is expected that such stationary discontinuity and, therefore, interior states are more common.

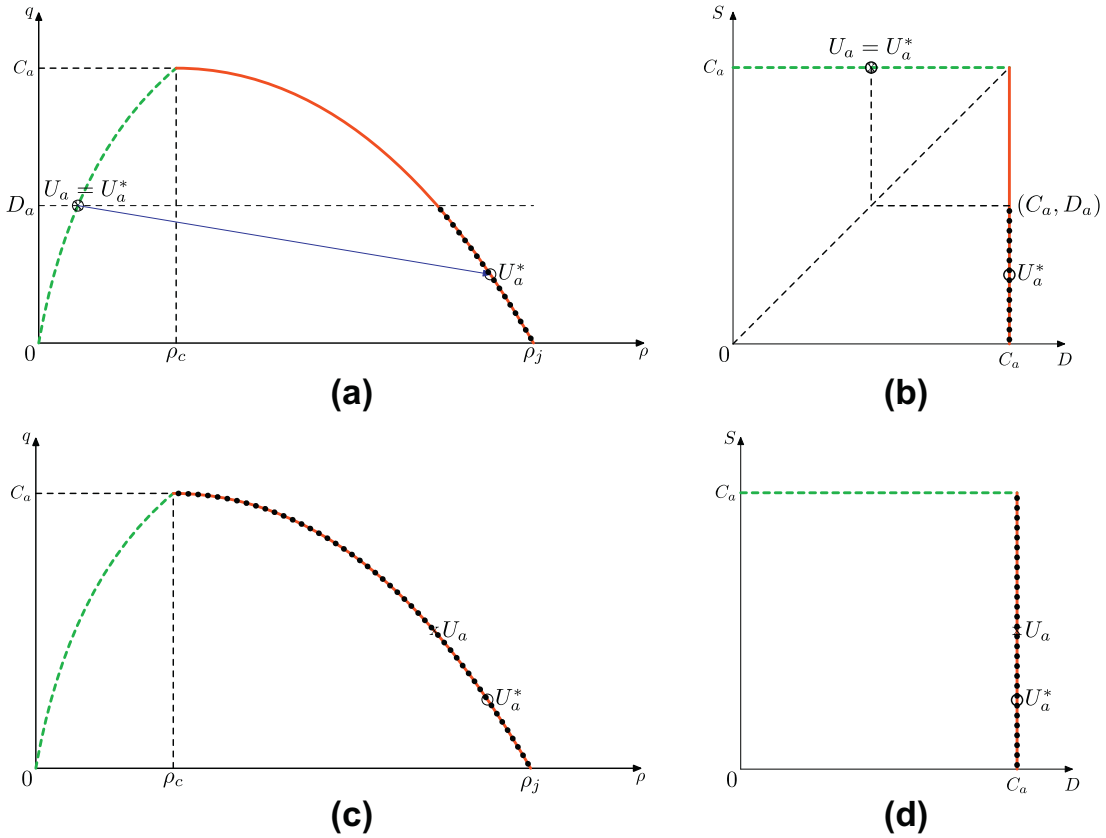

Fig. 5. Admissible stationary states (marked by black dots) for upstream link a: figures (a) and (c) are in density-flux space, and figures (b) and (d) are in supply-demand space.

where $S_a^* < D_a$, *and*

$$U_b^* = (C_b, S_b) \text{ or } (D_b^*, C_b), \tag{17b}$$

where $D_b^* < S_b$.

This lemma can be simply proved based on the observation that upstream waves cannot be positive and downstream waves cannot be negative with the LWR theory. We demonstrate the validity of this lemma with Fig. 5 for upstream stationary states and Fig. 6 for downstream stationary states in both density-flux and supply-demand spaces. In Fig. 5a and b, we can show the validity of (17a) when U_a is UC; i.e., when $D_a \leqslant S_a = C_a$: upstream link a has no kinematic wave when $U_a^* = U_a = (D_a, C_a)$ or a negative shock wave[2] when $U_a^* = (C_a, S_a^*)$ with $S_a^* < D_a$. In Fig. 5(c) and (d), we can show the validity of (17a) when U_a is SOC; i.e., when $S_a < D_a = C_a$: upstream link a has a negative shock or rarefaction wave when U_a^* is OC; i.e., $U_a^* = (D_a, C_a) = (C_a, C_a)$ or $(C_a, S_a^*)$with $S_a^* < D_a = C_a$. We can clearly see that, if U_a^* does not take values marked by black dots, the link would have positive shock or rarefaction waves. Therefore, (17a) is the sufficient and necessary conditions in order for kinematic waves on upstream link a to have negative speeds. Similarly, we can use Fig. 6 to demonstrate that (17b) is the sufficient and necessary conditions for downstream link b.

In addition, for interior states, we require that the Riemann problem for upstream link a with left and right initial conditions of U_a^* and U_a^0 cannot have negative waves, and the Riemann problem for downstream link b with left and right initial conditions of U_b^0 and U_b^* cannot have positive waves. Therefore, interior states U_a^0 and U_b^0 should satisfy the following admissible conditions in supply-demand space.

Lemma 3.2 (*Admissible interior states*). *For asymptotic stationary states* U_a^* *and* U_b^*, *interior states* U_a^0 *and* U_b^0 *are admissible if and only if*

$$U_a^0 = \begin{cases} (C_a, S_a^*) = U_a^*, & \text{when } U_a^* \text{ is SOC; i.e., } S_a^* < D_a^* = C_a \\ (D_a^0, S_a^0), & \text{when } U_a^* \text{ is UC; i.e., } D_a^* \leqslant S_a^* = C_a \end{cases} \tag{18a}$$

where $S_a^0 \geqslant D_a^*$, *and*

[2] Here we do not allow zero-speed shock waves either.

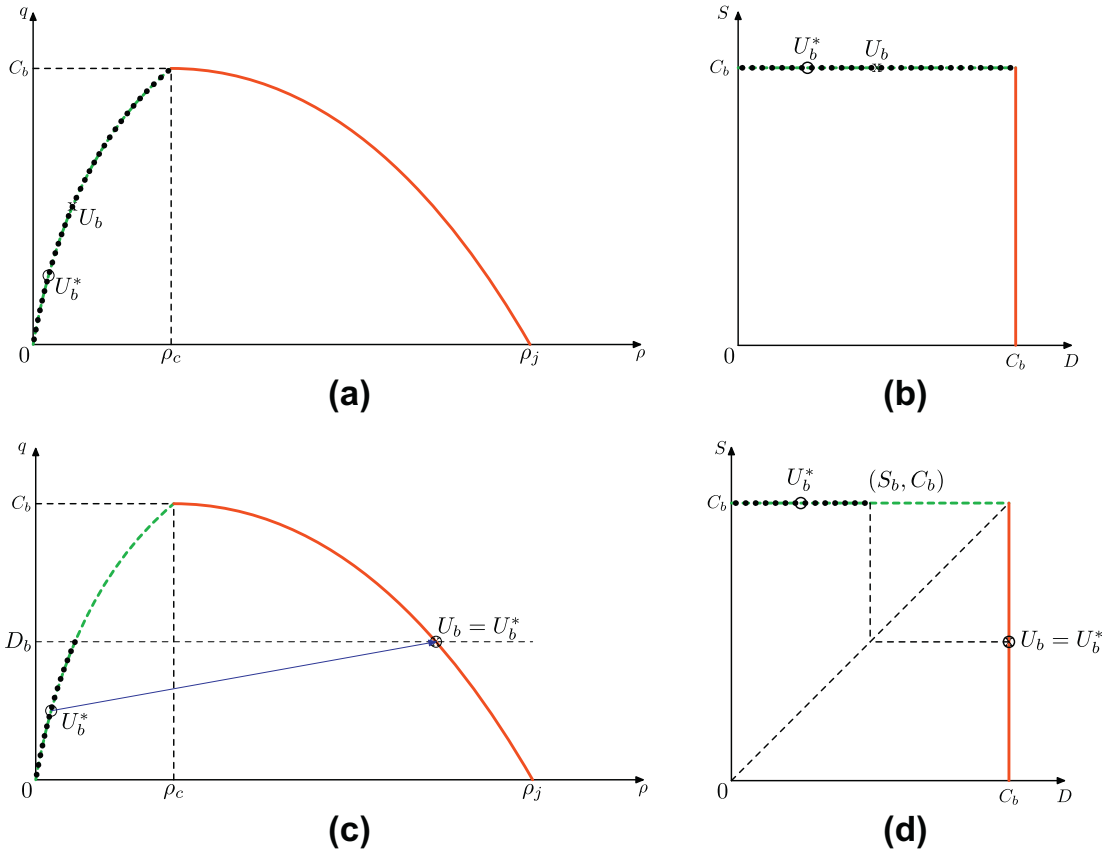

Fig. 6. Admissible stationary states for downstream link b: marked by black dots.

$$U_b^0 = \begin{cases} (D_b^*, C_b) = U_b^*, & \text{when } U_b^* \text{ is SUC; i.e., } D_b^* < S_b^* = C_b \\ \left(D_b^0, S_b^0\right), & \text{when } U_b^* \text{ is OC; i.e., } S_b^* \leqslant D_b^* = C_b \end{cases} \tag{18b}$$

where $D_b^0 \geqslant S_b^*$.

We denote a Riemann problem of the LWR model for link a with left and right initial conditions U_L and U_R by $LWR(U_L, U_R)$. Then we can summarize our first entropy condition in the following theorem.

Theorem 3.3 (*First entropy conditions*). *For the Riemann problem of (6) with initial conditions (10) for the junction in Fig. 2, we require that* $LWR(U_a, U_a^*)$ *can only have non-positive waves,* $LWR\left(U_a^*, U_a^0\right)$ *non-negative waves,* $LWR\left(U_b^0, U_b^*\right)$ *non-positive waves, and* $LWR(U_b^*, U_b)$ *non-negative waves. In supply-demand space, the feasible regions of stationary and interior states are given by*

$$\begin{aligned}
&U_a^* \in \mathbb{B}(U_a, \cdot) \equiv (D_a, C_a) \cup \left\{(C_a, S_a^*) \middle| S_a^* < D_a\right\}, \\
&U_a^0 \in \mathbb{F}(U_a^*, \cdot) \equiv \left\{(C_a, S_a^*) \middle| S_a^* < D_a^* = C_a\right\} \cup \left\{\left(D_a^0, S_a^0\right) \middle| S_a^0 \geqslant D_a^*, D_a^* \leqslant S_a^* = C_a\right\}, \\
&U_b^* \in \mathbb{F}(\cdot, U_b) \equiv (C_b, S_b) \cup \left\{(D_b^*, C_b) \middle| D_b^* < S_b\right\}, \\
&U_b^0 \in \mathbb{B}(\cdot, U_b^*) \equiv \left\{(D_b^*, C_b) \middle| D_b^* < S_b^* = C_b\right\} \cup \left\{\left(D_b^0, S_b^0\right) \middle| D_b^0 \geqslant S_b^*, S_b^* \leqslant D_b^* = C_b\right\}.
\end{aligned}$$

Therefore,

$$q_a \leqslant D_a \tag{19a}$$
$$q_b \leqslant S_b. \tag{19b}$$

In particular, U_a^* *is SOC if and only if* $q_a < D_a$ *and* $U_a^* = U_a^0 = (C_a, q_a)$; U_a^* *is UC if and only if* $q_a = D_a, U_a^* = (D_a, C_a)$, *and* $U_a^0 = \left(D_a^0, S_a^0\right)$ *with* $S_a^0 \geqslant D_a$. U_b^* *is SUC if and only if* $q_b < S_b$ *and* $U_b^* = U_b^0 = (q_b, C_b)$; U_b^* *is OC if and only if* $q_b = S_b, U_b^* = (C_b, S_b)$, *and* $U_b^0 = \left(D_b^0, S_b^0\right)$ *with* $D_b^0 \geqslant S_b$.

3.2. Fair merging and FIFO diverging rules in interior states

The first entropy conditions in Theorem 3.3 are not sufficient to pick out unique solutions of stationary states, since there can be many feasible stationary states for the same initial condition. In this subsection, we introduce an additional entropy condition, in which fair merging and FIFO diverging rules are used to prescribe boundary fluxes from interior states (Jin and Zhang, 2004):

1. Maximization of total flux:

$$\max q. \tag{20a}$$

2. Fair merging rule (Jin and Zhang, 2003b):

$$q_a = \frac{D_a^0}{\sum_{\alpha=1}^m D_\alpha^0} q. \tag{20b}$$

3. FIFO diverging rule (Papageorgiou, 1990; Daganzo, 1995b):

$$q_{a\to b} = \xi_{a\to b}^0 q_a,$$

which is equivalent to

$$q_b = \sum_{a=1}^m \xi_{a\to b}^0 q_a. \tag{20c}$$

4. Bounded fluxes: $q_a \in \left[0, D_a^0\right]$ and $q_b \in \left[0, S_b^0\right]$.

It was shown in (Jin and Zhang, 2004) that these entropy conditions lead to

$$q = \min_{b=m+1}^{m+n} \left\{ 1, \frac{S_b^0}{\sum_{a=1}^m D_a^0 \xi_{a\to b}^0} \right\} \sum_{a=1}^m D_a^0$$

$$q_{a\to b} = \frac{D_a^0 \xi_{a\to b}^0}{\sum_{\alpha=1}^m D_\alpha^0} q.$$

From (16a) and (20c), we can see that local turning proportions equal global turning proportions:

$$\xi_{a\to b}^0 = \xi_{a\to b}. \tag{21}$$

Therefore, we can simply replace $\xi_{a\to b}^0$ by $\xi_{a\to b}$ in the entropy conditions in (20).

As we know, in CTM fluxes through the junction shown in Fig. 2 are determined by the cells next to the junction. Thus the new entropy condition in (20) is consistent with the multi-commodity CTM in (Jin and Zhang, 2004).

4. Solutions to the Riemann problem for general junctions with fair merging and FIFO diverging rules

In this section, we solve stationary and interior states for the Riemann problem of the multi-commodity kinematic wave model, whose link-based version is given by (3) and (5) and path-based version by (6), with initial conditions in (10). Here we would like to first find fluxes in terms of initial demands, supplies, and turning proportions. That is, we want to find

$$q = F(\vec{D}, \vec{S}, \boldsymbol{\xi}),$$
$$q_a = F_a(\vec{D}, \vec{S}, \boldsymbol{\xi}), \quad a = 1, \ldots, m$$
$$q_b = F_b(\vec{D}, \vec{S}, \boldsymbol{\xi}), \quad b = m+1, \ldots, m+n$$

where $\vec{D} = (D_1, \ldots, D_m), \vec{S} = (S_{m+1}, \ldots, S_{m+n})$, and $\boldsymbol{\xi}(a, b) = \xi_{a\to b}$. Then from Theorem 3.3 we will be able to find corresponding stationary and interior states. Here fluxes, stationary states, and interior states should satisfy the two entropy conditions in the preceding section.

4.1. The fair merging rule and critical demand level

For upstream link $a = 1, \ldots, m$, we define its initial demand level by

$$\delta(a) = D_a / C_a. \tag{22}$$

Then we have Lemma 4.1.

Lemma 4.1. *For two upstream links a and α whose demand levels satisfy $\delta(a) \geqslant \delta(\alpha)$, (i) If U_a^* is UC then U_α^* is UC; (ii) If U_α^* is SOC then U_a^* is SOC. That is, the upstream link with a higher demand level is more prone to be congested.*

Proof. If U_a^* is UC, from Theorem 3.3 we have $q_a = D_a$. Then from the fair merging rule (20b) we have

$$\frac{q}{\sum_{i=1}^m D_i^0} = \frac{D_a}{D_a^0} \geqslant \delta(a),$$

since $D_a^0 \leqslant C_a$. Then $\delta(a) \geqslant \delta(\alpha)$ leads to

$$\frac{q}{\sum_{i=1}^m D_i^0} \geqslant \delta(\alpha).$$

Thus we conclude that upstream link α has to be UC. Otherwise, from Theorem 3.3 we have $q_\alpha < D_\alpha, D_\alpha^0 = C_\alpha$, and from (20b) we have

$$\frac{q}{\sum_{i=1}^m D_i^0} = \frac{q_\alpha}{C_\alpha} < \delta(\alpha),$$

which contradicts $\frac{q}{\sum_{i=1}^m D_i^0} \geqslant \delta(\alpha)$.

Conversely, if U_α^* is SOC then U_a^* is SOC. □

From Lemma 4.1, without loss of generality, we assume that initial demand levels of upstream links are ordered decreasingly: $\delta(1) \geqslant \delta(2) \geqslant \ldots \geqslant \delta(m)$. In addition, we can separate upstream links into two groups according to the criticality of their stationary states: the first $l (l = 0, \ldots, m)$ upstream links have SOC stationary states, and the remaining $m - l$ upstream links have UC stationary states. Thus from Theorem 3.3, we have

$$q_a < D_a^0 = C_a, \quad a = 1, \ldots, l \tag{23a}$$

$$q_\alpha = D_\alpha, \quad \alpha = l+1, \ldots, m \tag{23b}$$

Hereafter we call l a separation of criticality.

We define the critical demand level θ by

$$\theta = \frac{q}{\sum_{a=1}^l C_a + \sum_{\alpha=l+1}^m D_\alpha^0}. \tag{24}$$

From the entropy condition (20b) and (23) we have

$$q_a = \theta D_a^0 = \theta C_a, \quad a = 1, \ldots, l, \tag{25a}$$

$$q_\alpha = \theta D_\alpha^0 = D_\alpha, \quad \alpha = l+1, \ldots, m. \tag{25b}$$

Since $q_a < D_a$ for $a = 1, \ldots, l$ and $D_\alpha^0 \leqslant C_\alpha$ for $\alpha = l+1, \ldots, m$, we have

$$\delta(1) \geqslant \ldots \geqslant \delta(l) > \theta \geqslant \delta(l+1) \geqslant \ldots \geqslant \delta(m).$$

Therefore the condition above is a necessary condition for l to be a separation of criticality. On the other hand, the condition is also sufficient: if the inequality above is satisfied, we can have $q_a = \theta D_a^0 < \delta(a) C_a = D_a (a = 1, \ldots, l)$, which leads to SOC $U_a^* (a = 1, \ldots, l)$ from Theorem 3.3; in addition, U_{l+1}^* cannot be SOC, since, otherwise, $q_{l+1} < D_{l+1}$ contradicts $q_{l+1} = \theta D_{l+1}^0 = \theta C_{l+1} \geqslant D_{l+1}$. Therefore, l is a separation of criticality if and only if

$$\delta(l) > \theta \geqslant \delta(l+1). \tag{26}$$

Note that we ignore all conditions involving $\delta(0)$ or $\delta(m+1)$ in (26); i.e., $l = 0$ when $\theta \geqslant \delta(1)$, and $l = m$ when $\theta < \delta(m)$. From (26) we can define l as a function of critical demand level

$$l = L(\theta). \tag{27}$$

That is, for a given θ we can find a unique l such that (27) is satisfied. Obviously, l decreases with θ, and the inverse function does not exist.

If $l = L(\theta)$, from (24) we have

$$q = G(\theta, l) \equiv \theta \cdot \sum_{a=1}^{l} C_a + \sum_{\alpha=l+1}^{m} D_\alpha, \tag{28}$$

or equivalently

$$\theta = H(q, l) \equiv \frac{q - \sum_{\alpha=l+1}^m D_\alpha}{\sum_{a=1}^l C_a}. \tag{29}$$

Here we define

$$H(q,0)=\begin{cases}\infty & \text{when } q>\sum_{\alpha=1}^{m}D_\alpha\\ 1 & \text{when } q=\sum_{\alpha=1}^{m}D_\alpha\\ -\infty & \text{when } q<\sum_{\alpha=1}^{m}D_\alpha\end{cases} \tag{30}$$

Therefore, given initial upstream demands, q is a function of θ: $q = G(\theta, L(\theta))$. When $\theta \geqslant 1, q=\sum_{a=1}^{m}D_a$.

Lemma 4.2. *$q = G(\theta, L(\theta))$ is an increasing function of θ. Since q increases with θ, the flux maximization rule (20a) is equivalent to*

$$\max \theta \tag{31}$$

Proof. Assuming that $\theta_1 > \theta_2$, we have $l_1 = L(\theta_1) \leqslant l_2 = L(\theta_2)$. Then we have

$$q_1-q_2=G(\theta_1,l_1)-G(\theta_2,l_2)=(\theta_1-\theta_2)\sum_{a=1}^{l_1}C_a+\sum_{\alpha=l_1+1}^{l_2}(D_\alpha-\theta_2C_\alpha).$$

Since $\delta(\alpha) > \theta_2$ for $\alpha \leqslant l_2$, we have $q_1 - q_2 \geqslant 0$. Therefore q is an increasing function of θ, and (20a) is equivalent to (31). □

4.2. The FIFO diverging rule and an equivalent condition of flux optimization

For downstream link $b = m+1, \ldots, m+n$, we define $D_{a\to b} = D_a\xi_{a\to b}$, $C_{a\to b} = C_a\xi_{a\to b}$, and the initial supply level by $\sigma_b=\frac{S_b}{\sum_{a=1}^{m}D_a\xi_{a\to b}}$. For a critical demand level θ and the corresponding separation of criticality $l (l = 0, \ldots, m)$, from (20c), (25), and (29) , we have for downstream link b

$$q_b=\sum_{a=1}^{m}q_a\xi_{a\to b}=\sum_{a=1}^{l}\theta C_{a\to b}+\sum_{\alpha=l+1}^{m}D_{\alpha\to b}, \tag{32}$$

where $l = L(\theta)$. Since $q_b \leqslant S_b$, we have

$$\theta\leqslant\gamma_b(l),\quad b=m+1,\ldots,m+n, \tag{33}$$

where the supply level of link b, $\gamma_b(l)$, is defined by

$$\gamma_b(l)=\frac{S_b-\sum_{\alpha=l+1}^{m}D_{\alpha\to b}}{\sum_{a=1}^{l}C_{a\to b}}. \tag{34}$$

Note that when $l = 0$ we define

$$\gamma_b(0)=\begin{cases}\infty, & S_b>\sum_{\alpha=1}^{m}D_{\alpha\to b}\\ 1, & S_b=\sum_{\alpha=1}^{m}D_{\alpha\to b}\\ -\infty, & S_b<\sum_{\alpha=1}^{m}D_{\alpha\to b}\end{cases}$$

We have that $\sigma_b = \gamma_b(m)$. That is, the initial supply level equals the supply level when all upstream links carry SOC stationary states.

Therefore, entropy conditions in (20) have been reduced to an optimization problem of critical demand level θ, (31), s.t. (33) and $l = L(\theta)$. Here, $l = L(\theta)$ is equivalent to the fair merging rule (20b), and (33) is equivalent to the FIFO diverging rule (20c). Obviously $\theta = 0$ is in the feasible region defined by $l = L(\theta)$ and (33): When $\theta = 0$, then $l = L(0)$, $D_a > 0$ for $a = 1, \ldots, l$, and $D_\alpha = 0$ for $\alpha = l+1, \ldots, m$; then $\gamma_b(l)=S_b/\sum_{a=1}^{l}C_{a\to b}>0=\theta$, and (33) is satisfied.

4.3. Existence and uniqueness of critical demand level

In this subsection, we establish that, given initial conditions $\vec{D}, \vec{S}$, and ξ, there exists a unique critical demand level, θ. First we study the pattern of supply levels $\gamma_b(a)$ for any $b = m+1, \ldots, m+n$ and $a = 1, \ldots, m$.

Lemma 4.3. *If $\gamma_b(l) \geqslant \delta(l)$ for $l = 1, \ldots, m-1$, then $\gamma_b(l) \geqslant \gamma_b(l+1) \geqslant \delta(l+1)$; If $\gamma_b(l) < \delta(l)$ for $l = 2, \ldots, m$, then $\gamma_b(l-1) < \gamma_b(l) < \delta(l) \leqslant \delta(l-1)$. That is, if the supply level is greater than the demand level at some link number, l, then supply levels will be decreasing and always greater than the corresponding demand levels for larger link numbers; on the other hand, if the supply level is strictly smaller than the demand level at some link number, l, then supply levels will be strictly increasing and always strictly smaller than the corresponding demand levels for smaller link numbers.*

Proof. If $\gamma_b(l) \geqslant \delta(l) \geqslant \delta(l+1)$, we have from the definition in (34)

$$\gamma_b(l+1)=\frac{S_b-\sum_{\alpha=l+1}^{m}D_{\alpha\to b}+D_{l+1\to b}}{\sum_{a=1}^{l+1}C_{a\to b}}=\frac{\gamma_b(l)\sum_{a=1}^{l}C_{a\to b}+\delta(l+1)C_{l+1\to b}}{\sum_{a=1}^{l+1}C_{a\to b}}\leqslant\frac{\gamma_b(l)\sum_{a=1}^{l}C_{a\to b}+\gamma_b(l)C_{l+1\to b}}{\sum_{a=1}^{l+1}C_{a\to b}}=\gamma_b(l).$$

In addition, we have

$$(\gamma_b(l+1)-\delta(l+1))\sum_{a=1}^{l+1}C_{a\to b}=\gamma_b(l)\sum_{a=1}^{l}C_{a\to b}+\delta(l+1)C_{l+1\to b}-\delta(l+1)\sum_{a=1}^{l}C_{a\to b}-\delta(l+1)C_{l+1\to b}$$

$$=(\gamma_b(l)-\delta(l+1))\sum_{a=1}^{l}C_{a\to b}\geqslant 0,$$

since $\gamma_b(l)\geqslant\delta(l+1)$. Therefore, $\gamma_b(l)\geqslant\gamma_b(l+1)\geqslant\delta(l+1)$ when $\gamma_b(l)\geqslant\delta(l+1)$.

If $\gamma_b(l)<\delta(l)$, we have from the definition in (34)

$$\gamma_b(l-1)=\frac{S_b-\sum_{\alpha=l+1}^{m}D_{\alpha\to b}-D_{l\to b}}{\sum_{a=1}^{l-1}C_{a\to b}}=\frac{\gamma_b(l)\sum_{a=1}^{l}C_{a\to b}-\delta(l)C_{l\to b}}{\sum_{a=1}^{l-1}C_{a\to b}}<\frac{\gamma_b(l)\sum_{a=1}^{l}C_{a\to b}-\gamma_b(l)C_{l\to b}}{\sum_{a=1}^{l-1}C_{a\to b}}=\gamma_b(l).$$

Therefore, $\gamma_b(l-1)<\gamma_b(l)<\delta(l)\leqslant\delta_{l-1}$ when $\gamma_b(l)<\delta(l)$. □

Since $\gamma_b(a)$ is either greater than or strictly smaller than $\delta(a)$ for any upstream link a, Lemma 4.3 means that either the supply levels for links smaller than a are strictly increasing or those for links larger than a are decreasing. Then we have the following patterns for all supply levels.

Lemma 4.4. *For downstream link b, its supply levels $\gamma_b(l)$ ($l=0,\dots,m$) follows one and only one of the following patterns:*

1. *When $S_b\geqslant\sum_{\alpha=1}^{m}D_{\alpha\to b}$, $\gamma_b(l)\geqslant\delta(l)$ for $l=1,\dots,m$, and $\gamma_b(0)\geqslant\cdots\geqslant\gamma_b(m)$. That is, all supply levels are decreasing.*
2. *When $S_b<\sum_{\alpha=1}^{m}D_{\alpha\to b}$ and $\gamma_b(m)<\delta(m)$, $\gamma_b(l)<\delta(l)$ for $l=1,\dots,m$, and $\gamma_b(0)<\cdots<\gamma_b(m)$. That is, all supply levels are strictly increasing.*
3. *There exists a unique $l=1,\dots,m-1$, such that*

$$\gamma_b(l)<\delta(l),\quad \gamma_b(l+1)\geqslant\delta(l+1), \tag{35a}$$

or equivalently

$$\gamma_b(0)<\ldots<\gamma_b(l)\geqslant\gamma_b(l+1)\geqslant\ldots\geqslant\gamma_b(m), \tag{35b}$$

or equivalently

$$\delta(l)>\gamma_b(l)\geqslant\delta(l+1). \tag{35c}$$

That is, supply levels first strictly increase and then decrease.

If we ignore all conditions involving $\delta(0)$ and $\delta(m+1)$, we can conclude that, for any $\gamma_b(l)$, there exists one and only one $l=0,\dots,m$ such that (35a), (35b), and (35c) are satisfied. Furthermore, l is the smallest solution of

$$\gamma_b(l)=\max_k\gamma_b(k). \tag{35d}$$

Proof.

1. It is straightforward to show that $\gamma_b(1)\geqslant\delta(1)$ is equivalent to $S_b\geqslant\sum_{\alpha=1}^{m}D_{\alpha\to b}$. Then Lemma 4.3 implies that $\gamma_b(l)\geqslant\delta(l)$ for $l=1,\dots,m$, and $\gamma_b(1)\geqslant\ldots\geqslant\gamma_b(m)$. In this case, supply levels are decreasing.
2. Otherwise, $S_b<\sum_{\alpha=1}^{m}D_{\alpha\to b}$, or equivalently $\gamma_b(1)<\delta(1)$. Further if $\gamma_b(m)<\delta(m)$, Lemma 4.3 implies that $\gamma_b(l)<\delta(l)$ for $l=1,\dots,m$, and $\gamma_b(0)<\cdots<\gamma_b(m)$. In this case, supply levels are strictly increasing.
3. Otherwise, $\gamma_b(1)<\delta(1)$ and $\gamma_b(m)\geqslant\delta(m)$. In this case, there exists one and only one $l(1\leqslant l\leqslant m-1)$ such that (35a) is satisfied.
   (a) We assume that no l satisfies that $\gamma_b(l)<\delta(l)$ and $\gamma_b(l+1)\geqslant\delta(l+1)$. Then for all $l=1,\dots,m-1$, either $\gamma_b(l)\geqslant\delta(l)$ or $\gamma_b(l+1)<\delta(l+1)$. Since we have $\gamma_b(1)<\delta(1)$, then we must have $\gamma_b(2)<\delta(2)$. By repeating the argument, we must have $\gamma_b(l+1)<\delta(l+1)$ for $l=1,\dots,m-1$, which contradicts $\gamma_b(m)\geqslant\delta(m)$. Hence, there exists at least one $l(1\leqslant l\leqslant m-1)$ such that (35a) is satisfied.
   (b) We assume that there exists l_1 and $l_2(1\leqslant l_1<l_2\leqslant m-1)$, such that $\gamma_b(l_1)<\delta(l_1)$, $\gamma_b(l_1+1)\geqslant\delta(l_1+1)$, $\gamma_b(l_2)<\delta(l_2)$, and $\gamma_b(l_2+1)\geqslant\delta(l_2+1)$. From $\gamma_b(l_2)<\delta(l_2)$, Lemma 4.3 implies that $\gamma_b(l_1+1)\leqslant\gamma_b(l_2)<\delta(l_2)\leqslant\delta(l_1+1)$, since $l_1+1\leqslant l_2$. This contradicts $\gamma_b(l_1+1)\geqslant\delta(l_1+1)$. Hence, there exists only one $l(1\leqslant l\leqslant m-1)$ such that (35a) is satisfied.

We can see that, in this case, supply levels first increase and then decrease.

Next we prove that (35a), (35b), and (35c) are equivalent:

1. If (35a) is satisfied, we have

$$\gamma_b(l+1)=\frac{\gamma_b(l)\sum_{a=1}^{l}C_{a\to b}+\delta(l+1)C_{l+1\to b}}{\sum_{a=1}^{l+1}C_{a\to b}}\leqslant\frac{\gamma_b(l)\sum_{a=1}^{l}C_{a\to b}+\gamma_b(l+1)C_{l+1\to b}}{\sum_{a=1}^{l+1}C_{a\to b}}.$$

Hence $\gamma_b(l)\geqslant\gamma_b(l+1)$. From Lemma 4.3, we can conclude that (35a) implies (35b).

2. From (35b) we have $\gamma_b(l)\geqslant\gamma_b(l+1)$. Thus

$$\gamma_b(l+1)=\frac{\gamma_b(l)\sum_{a=1}^{l}C_{a\to b}+\delta(l+1)C_{l+1\to b}}{\sum_{a=1}^{l}C_{a\to b}+C_{l+1\to b}}\leqslant\gamma_b(l),$$

which leads to $\gamma_b(1+1)\geqslant\delta(l+1)$. If $l=1$, it is assumed that $\gamma_b(l)<\delta(l)$. If $l>1$, we have from (35b) that $\gamma_b(l)>\gamma_b(l-1)$. Thus

$$\gamma_b(l-1)=\frac{\gamma_b(l)\sum_{a=1}^{l}C_{a\to b}-\delta(l)C_{l\to b}}{\sum_{a=1}^{l}C_{a\to b}-C_{l\to b}}<\gamma_b(l),$$

which leads to $\gamma_b(l)<\delta(l)$. Therefore, (35b) implies (35c).

3. If (35c) is satisfied, we have

$$\gamma_b(l+1)=\frac{\gamma_b(l)\sum_{a=1}^{l}C_{a\to b}+\delta(l+1)C_{l+1\to b}}{\sum_{a=1}^{l+1}C_{a\to b}}\geqslant\frac{\gamma_b(l+1)\sum_{a=1}^{l}C_{a\to b}+\delta(l+1)C_{l+1\to b}}{\sum_{a=1}^{l+1}C_{a\to b}},$$

which leads to $\gamma_b(l+1)\geqslant\delta(l+1)$. That is, (35a) is satisfied.

Furthermore, we can unify the three cases such that (35a)–(35c) and (35d) serve as necessary and sufficient conditions for Case 1 when $l=0$, and for Case 2 when $l=m$. In other words, there exists one and only one $l=0,\dots,m$ such that (35a)–(35c) and (35d) are satisfied. □

We define minimum supply levels over all downstream links for $l=0,\dots,m$ as

$$\Gamma(l)\equiv\min_b\gamma_b(l). \tag{36}$$

Lemma 4.5. *If $\Gamma(l)\geqslant\delta(l)$ for any $l=1,\dots,m-1$, then $\Gamma(l)\geqslant\Gamma(l+1)\geqslant\delta(l+1)$; If $\Gamma(l)<\delta(l)$ for any $l=2,\dots,m$, then $\Gamma(l-1)<\Gamma(l)<\delta(l)\leqslant\delta(l-1)$. That is, minimum supply levels have the same pattern as supply levels of individual downstream links.*

Proof. If $\Gamma(l)\geqslant\delta(l)$, then $\gamma_b(l)\geqslant\delta(l)$ for all b. Lemma 4.3 implies that $\gamma_b(l)\geqslant\gamma_b(l+1)\geqslant\delta(l+1)$ for all b. Then $\min_b\gamma_b(l)\geqslant\min_b\gamma_b(l+1)\geqslant\delta(l+1)$. That is, $\Gamma(l)\geqslant\Gamma(l+1)\geqslant\delta(l+1)$.

If $\Gamma(l)<\delta(l)$ for $l=2,\dots,m$, then there exists at least one b, such that $\gamma_b(l)<\delta(l)$. Lemma 4.3 implies that $\gamma_b(l-1)<\gamma_b(l)<\delta(l)$ and $\gamma_b(l-1)<\delta(l)\leqslant\gamma_\beta(l)$ for all b that satisfies $\gamma_b(l)<\delta(l)$ and all β that satisfies $\gamma_\beta(l)\geqslant\delta(l)$. Therefore

$$\Gamma(l-1)=\min_b\gamma_b(l-1)\leqslant\min_{b:\gamma_b(l)<\delta(l)}\gamma_b(l-1)<\min_b\gamma_b(l)=\Gamma(l)<\delta(l)\leqslant\delta(l+1).$$

□

Lemma 4.6. *For given $\vec{D},\vec{C},\vec{S}$, and ξ, there exists one and only one $l=0,\dots,m$ such that*

$$\Gamma(l)<\delta(l),\quad\Gamma(l+1)\geqslant\delta(l+1), \tag{37a}$$

which is equivalent to one of the following conditions:

$$\Gamma(0)<\cdots<\Gamma(l)\geqslant\Gamma(l+1)\geqslant\cdots\geqslant\Gamma(m), \tag{37b}$$

$$\delta(l)>\Gamma(l)\geqslant\delta(l+1). \tag{37c}$$

Here l is also the smallest solution of

$$\Gamma(l)=\max_k\Gamma(k). \tag{37d}$$

Note that here all conditions involving $\delta(0)$ and $\delta(m+1)$ are ignored.

Proof. This is a direct result of Lemmas 4.4 and 4.5, and the proof is omitted. □

Now we are ready to prove the existence and uniqueness of the critical demand level θ.

Theorem 4.7. *For given initial conditions $\vec{D}, \vec{C}, \vec{S}$, and ξ, solutions of the critical demand level, θ, and the separation of criticality, l, exist and are unique. In particular, they solve the following equations*

$$\theta = \Gamma(l), \tag{38a}$$
$$l = L(\theta). \tag{38b}$$

Equivalently, θ solves the following max–min problem

$$\theta = \max_{k=0}^{m} \Gamma(k) = \max_{k=0}^{m} \min_{b=m+1}^{m+n} \gamma_b(k) = \min_{b=m+1}^{m+n} \max_{k=0}^{m} \gamma_b(k), \tag{39}$$

and $l = L(\theta)$.

Proof. From the definition of $l = L(\theta)$, we have that

$$\delta(l) > \theta \geqslant \delta(l+1).$$

Since $\theta = \Gamma(l)$, we can eliminate θ to obtain

$$\delta(l) > \Gamma(l) \geqslant \delta(l+1).$$

Lemma 4.6 implies that there exists a unique l satisfying the equation above, which is the same as (37c). That is, there exists a unique solutions of l and θ for the equations

$$\theta = \Gamma(l),$$
$$l = L(\theta).$$

Furthermore, from Lemma 4.6, $\theta = \Gamma(l)$ is equivalent to (39). □

From Theorem 4.7 we have the following special case.

Corollary 4.8. (*A special case*) *The following statements are equivalent*

1. *All upstream stationary states are UC.*
2. *$l = 0$.*
3. *$\theta \geqslant 1$.*
4. *$q = \sum_{a=1}^{m} D_a$.*
5. *$S_b \geqslant \sum_{a=1}^{m} D_{a\to b}$ for all b.*
6. *$\gamma_b(l)$ decreases in l for all b.*
7. *$\gamma_b(1) \geqslant \delta(1)$ for all b.*

4.4. Solutions of stationary states, interior states, and kinematic waves on all links

From the preceding subsection, we find that the critical demand level is determined by upstream demands and capacities, downstream supplies, and diverging proportions. That is, when upstream demand levels are ordered $\delta(1) \geqslant \cdots \geqslant \delta(m)$, we have

$$\theta = \max_{k=0}^{m} \min_{b=m+1}^{m+n} \frac{S_b - \sum_{\alpha=k+1}^{m} D_\alpha \xi_{\alpha\to b}}{\sum_{a=1}^{k} C_a \xi_{a\to b}}, \tag{40a}$$

and $l = L(\theta)$. Once we find θ and l, we can calculate fluxes through the junction as follows. The total flux can be computed as

$$q = \sum_{a=1}^{l} \theta C_a + \sum_{\alpha=l+1}^{m} D_\alpha. \tag{40b}$$

For upstream links we have ($a = 1, \ldots, m$)

$$q_a = \min\{D_a, \theta C_a\}. \tag{40c}$$

In this sense,

$$\widetilde{S}_a \equiv \theta C_a$$

can be considered as the downstream supply of link a, such that

$$q_a = \min\{D_a, \widetilde{S}_a\}.$$

For downstream links we have ($b = m+1, \ldots, m+n$)

$$q_b = \sum_{a=1}^{l} \theta C_a \xi_{a\to b} + \sum_{\alpha=l+1}^{m} D_\alpha \xi_{\alpha\to b} = \min_{\beta=m+1}^{m+n} \sum_{a=1}^{l} C_a \xi_{a\to b} \gamma_\beta(l) + \sum_{\alpha=l+1}^{m} D_\alpha \xi_{\alpha\to b}$$
$$= \min\left\{ S_b, \min_{\beta=m+1,\beta\neq b}^{m+n} \sum_{a=1}^{l} C_a \xi_{a\to b} \gamma_\beta(l) + \sum_{\alpha=l+1}^{m} D_\alpha \xi_{\alpha\to b} \right\}. \quad (40d)$$

In this sense,

$$\widetilde{D}_b \equiv \min_{\beta=m+1,\beta\neq b}^{m+n} \sum_{a=1}^{l} C_a \xi_{a\to b} \gamma_\beta(l) + \sum_{\alpha=l+1}^{m} D_\alpha \xi_{\alpha\to b}$$

can be considered as the upstream demand of link b, such that

$$q_b = \min\{\widetilde{D}_b, S_b\}.$$

Then following Theorem 3.3, we can find the corresponding stationary and interior states for all links. For $a = 1, \ldots, l$, demand level of link a is greater than the critical demand level, $q_a = \theta C_a$, and its stationary state is SOC with $U_a^* = (C_a, \theta C_a)$; for $\alpha = l+1, \ldots, m$, demand level of link α is not greater than the critical demand level, $q_\alpha = D_\alpha$, and its stationary state is UC with $U_\alpha^* = (D_\alpha, C_\alpha)$. For $a = 1, \ldots, l$, link a does not have an interior state, or $U_a^0 = U_a^*$; but for $\alpha = l+1, \ldots, m$, the transitional state should satisfy (20b), which leads to $q_\alpha = D_\alpha^0 \theta = D_\alpha$. Then

$$D_\alpha^0 = D_\alpha/\theta.$$

Theorem 3.3 implies that $U_\alpha^0 = \left(D_\alpha/\theta, S_\alpha^0\right)$ with $S_\alpha^0 \geqslant D_\alpha$ and $\max\left\{S_\alpha^0, D_\alpha/\theta\right\} = C_\alpha$. For downstream link b, we can similarly determine its stationary and interior states.

From the stationary state on a link, we can calculate its stationary density ρ_a^* and ρ_b^* from (9). Then we can obtain kinematic waves on all upstream and downstream links by solving (11) with initial conditions (12) and (13) with initial conditions (14), respectively. Since stationary states are unique, such kinematic waves are also unique.

In the following, we consider some special junctions:

1. For a linear junction with $m = n = 1, \xi_{1\to 2} = 1$. When $S_2 \geqslant D_1$, $\theta = 1, l = 0$, and $q_1 = q_2 = q = D_1$; when $S_2 < D_1$, $\theta = S_2/C_1$, $l = 1$, and $q_1 = q_2 = q = S_2$. This is consistent with $q = \min\{D_1, S_2\}$ (Daganzo, 1995b; Lebacque, 1996).
2. For a merging junction with $m > 1$ and $n = 1, \xi_{a\to m+1} = 1$. Then

$$\theta = \max_{k=0}^{m} \frac{S_{m+1} - \sum_{\alpha=k+1}^{m} D_\alpha}{\sum_{a=1}^{k} C_a},$$

and $l = L(\theta)$. Obviously, when $S_{m+1} \geqslant \sum_{\alpha=1}^{m} D_\alpha$; i.e., the downstream supply is greater than the sum of upstream demands, $\theta \geqslant 1, l = 0, q_a = D_a$, and all upstream links have UC stationary states. In particular, when $m = 2$,

$$\theta = \max\{\gamma_3(0), \gamma_3(1), \gamma_3(2)\} = \max\left\{\gamma_3(0), \frac{S_3 - D_2}{C_1}, \frac{S_3}{C_1 + C_2}\right\},$$

where $\gamma_3(0) = 1$ when $S_3 \geqslant D_1 + D_2$ or $-\infty$ otherwise. Thus solutions of (q_1, q_2) are

$$(q_1, q_2) = \begin{cases} (D_1, D_2), & S_3 \geqslant D_1 + D_2 \\ (S_3 - D_2, D_2), & \frac{C_1}{C_1+C_2} S_3 \leqslant S_3 - D_2 < D_1 \\ \left(\frac{C_1}{C_1+C_2} S_3, \frac{C_2}{C_1+C_2} S_3\right), & S_3 - D_2 < \frac{C_1}{C_1+C_2} S_3 < D_1 \end{cases}$$

which is consistent with solutions of the fair merge model (Jin, 2010c):

$$q_1 = \min\left\{D_1, \max\left\{S_3 - D_2, \frac{C_1}{C_1 + C_2} S_3\right\}\right\},$$
$$q_2 = \min\left\{D_2, \max\left\{S_3 - D_1, \frac{C_2}{C_1 + C_2} S_3\right\}\right\}.$$

Note that here $D_1/C_1 \geqslant D_2/C_2$, which is not required in the model above.

3. For a diverging junction with $m = 1$ and $n > 1$,

$$\theta = \min_{b=2}^{1+n} \max\left\{\gamma_b(0), \frac{S_b}{C_1 \xi_{1\to b}}\right\},$$

where $\gamma_b(0) = 1$ when $S_b \geqslant D_1 \xi_{1\to b}$ or $-\infty$ otherwise. Thus solutions of q_1 are

$$q_1 = \begin{cases} D_1, & \frac{S_b}{C_1 \xi_{1\to b}} \geqslant \frac{D_1}{C_1} \forall b \\ \min\limits_{b=2}^{1+n} \frac{S_b}{\xi_{1\to b}}, & \min\limits_{b=2}^{1+n} \frac{S_b}{C_1 \xi_{1\to b}} < \frac{D_1}{C_1} \end{cases}$$

which is consistent with solutions of the FIFO diverge model (Jin, 2010b):

$$q_1 = \min_{b=2}^{1+n} \left\{ D_1, \frac{S_b}{\xi_{1\to b}} \right\}.$$

5. A simple model of general intersections

For a general intersection with four upstream and four downstream links,[3] there are totally 16 traffic streams, which can have no conflicts, diverging conflicts, merging conflicts, or crossing conflicts between each other. In this section, we only consider merging and diverging conflicts and model the intersection as a general junction with four upstream links and four downstream links shown in Fig. 7. In this network, east–west streets, links 1, 2, 5, and 6, are major roads with two lanes; north–south streets, links 3, 4, 7, and 8, are minor roads with one lane.

For the major roads, their fundamental diagram (Del Castillo and Benitez, 1995) is ($\rho \in [0, 2\rho_j]$)

$$V(\rho) = \rho v_{f,1} \left\{ 1 - \exp\left[1 - \exp\left(\frac{|C_j|}{v_{f,1}} \left(\frac{2\rho_j}{\rho} - 1 \right) \right) \right] \right\},$$

where the free flow speed $v_{f,1}$ = 80 km/h, the shock wave velocity at jam density C_j = − 20 km/h, and jam density ρ_j = 150 veh/km. For the minor roads, their fundamental diagram is ($\rho \in [0, \rho_j]$)

$$Q(\rho) = v_{f,2} \rho \left\{ 1 - \exp\left[1 - \exp\left(\frac{|C_j|}{v_{f,2}} \left(\frac{\rho_j}{\rho} - 1 \right) \right) \right] \right\},$$

where $v_{f,2}$ = 60 km/h. Thus the critical density and capacity of the major roads are $\rho_{c,1}$ = 73 veh/km and C_1 = 4038 veh/h, and those of the minor roads are $\rho_{c,2}$ = 43 veh/km and C_2 = 1871 veh/h.

In the following example, initial traffic densities on links 1 to 8 are 41.3195, 35.4850, 18.7149, 15.5944, 50, 178.2464, 30, and 73.5029 veh/km, respectively. Thus all upstream links and downstream links except links 6 and 8 are initially UC, and downstream links 6 and 8 are initially SOC. The corresponding demands of the four upstream links are $0.8C_1$, $0.7C_1$, $0.6C_2$, and $0.5C_2$, respectively; and the supplies of the four downstream links are C_1, $0.6C_1$, C_2, and $0.8C_2$, respectively. The turning proportions matrix is time-independent and given by

$$\xi = \begin{bmatrix} 0.1 & 0.6 & 0.2 & 0.1 \\ 0.6 & 0.1 & 0.1 & 0.2 \\ 0.2 & 0.2 & 0.1 & 0.5 \\ 0.2 & 0.2 & 0.5 & 0.1 \end{bmatrix}.$$

5.1. Theoretical solutions

From the initial conditions, we can see that the demand levels for upstream links are δ = [0.8, 0.7, 0.6, 0.5], which are already ordered. From Theorem 4.7 and procedures in (40), we can calculate a critical demand level θ = 0.6952 and the separation of criticality l = 2. Therefore, stationary states on links 1 and 2 are SOC, and those on links 3 and 4 are UC. Then the total flux through the intersection is q = 7671 veh/h; out-fluxes of upstream links are 0.6952 C_1, 0.6952 C_1, 0.6 C_2, and 0.5 C_2 for links 1–4, respectively; in-fluxes of downstream links are 0.5886 C_1, 0.5886 C_1, 0.76 C_2, and 0.8 C_2 for links 5 to 8, respectively. Then from Theorem 3.3, we can find the stationary states and interior states as follows:

1. Both links 1 and 2 are stationary at SOC with the same stationary and interior states $U_1^* = U_2^* = U_1^0 = U_2^0 = (1, 0.6952)C_1$. The corresponding densities are $\rho_1^* = \rho_2^* = \rho_1^0 = \rho_2^0 = 158.4133$ veh/km.
2. Both links 3 and 4 are UC with stationary states: $U_3^* = U_3 = (0.6, 1)C_2$, and $U_4^* = U_4 = (0.5, 1)C_2$. The corresponding densities are $\rho_3^* = 18.7149$ veh/km, and $\rho_4^* = 15.5944$ veh/km. Their interior states are $U_3^0 = (0.8631, 1)C_2$, and $U_4^0 = (0.7193, 1)C_2$. The corresponding densities are $\rho_3^0 = 27.9709$ veh/km, and $\rho_4^0 = 22.5162$ veh/km.
3. Links 5, 6, and 7 are stationary at UC with $U_5^* = U_6^* = U_5^0 = U_6^0 = (0.5885, 1)C_1$, and $U_7^* = U_7^0 = (0.76, 1)C_2$. The corresponding densities are $\rho_5^* = \rho_5^0 = \rho_6^* = \rho_6^0 = 29.7122$ veh/km, and $\rho_7^* = \rho_7^0 = 23.8991$ veh/km.
4. Link 8 is stationary at SOC with $U_8^* = U_8^0 = U_8 = (1, 0.8)C_2$. The corresponding densities are $\rho_8^* = \rho_8^0 = 73.5029$ veh/km.

[3] Such an intersection can be considered as an approximation of an urban or freeway intersection with multiple upstream and downstream links.

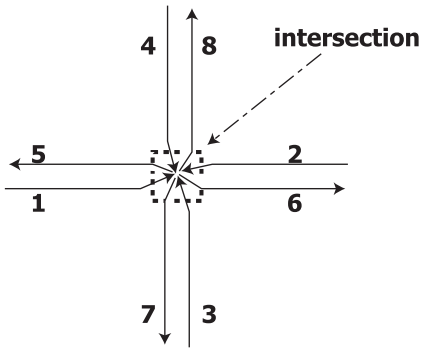

Fig. 7. A four by four intersection.

Thus we can see that the bottleneck in this network is link 8: link 8 remains congested, queues back up on upstream links 1 and 2, and free flows form on downstream links 5, 6, and 7. Then by solving (11) with initial conditions (12) and (13) with initial conditions (14), we find the following kinematic waves:

1. On links 1 and 2, there are backward shock waves. The shock wave speeds are −3.6157 km/h and −0.1592 km/h, respectively.
2. On links 3 and 4, there are no waves.
3. On links 5, 6, and 7, there are forward shock waves. The shock wave speeds are 63.6780 km/h, 0.3109 km/h, and 43.8685 km/h.
4. On link 8, there is no wave.

The aforementioned initial conditions, stationary states, interior states, and shock waves are shown in Fig. 8. In Fig. 8a, solutions of four upstream links are shown in $\rho - q$ space with two fundamental diagrams. In the figure we can see two backward shock waves on links 1 and 2. In Fig. 8b, solutions of four downstream links are shown. In the figure we can see three forward shock waves on links 5, 6, and 7.

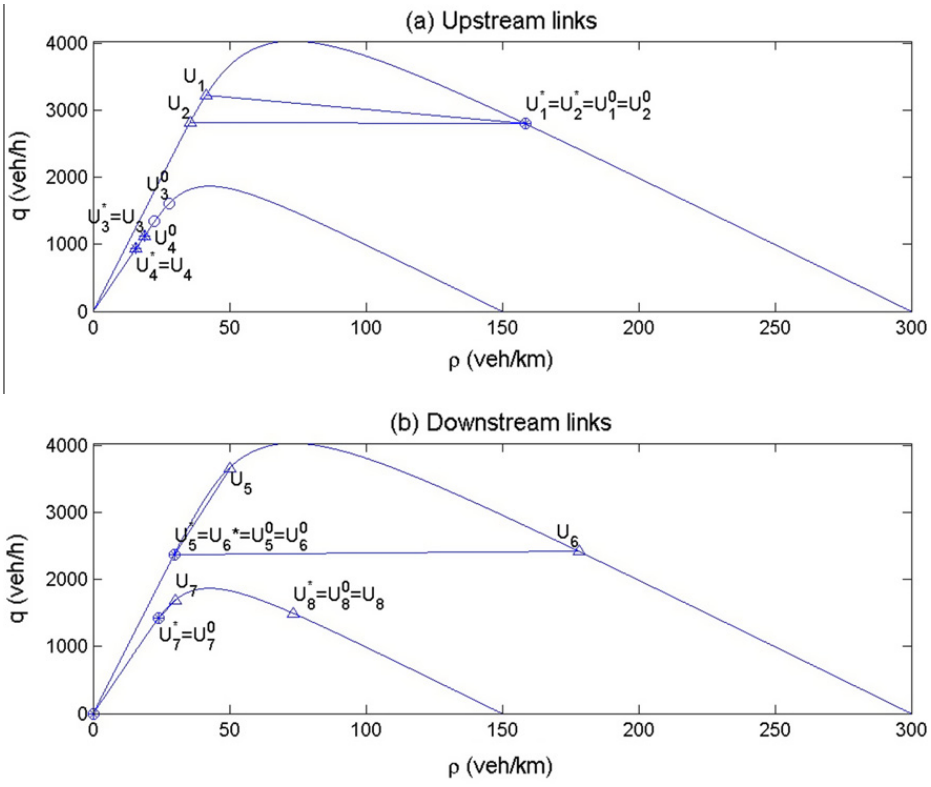

Fig. 8. Theoretical solutions of traffic dynamics at a 4 × 4 intersection.

5.2. Numerical solutions

In this subsection, we numerically solve traffic dynamics in Fig. 7 with the same initial and boundary conditions by using the multi-commodity CTM with fair merging and FIFO diverging rules (Jin and Zhang, 2004). Here all links have finite lengths, and we use the following boundary conditions: for upstream links, their upstream demands are the same as respective initial demands; for downstream links, their downstream supplies are the same as respective initial supplies. In numerical solutions, the simulation time duration is $T = 0.5$ h, and the lengths of links 1 to 8 are set as 2, 0.1, 0.5, 0.5, 30, 0.2, 20, 0.5 km, respectively. We discretize each link into a number of cells and divide the simulation time duration T into N steps. We set cell size $\Delta x = 0.01$ km and time step-size $\Delta t = 0.000125$ h, which satisfy the CFL condition (Courant et al., 1928): $v_{f,1}\frac{\Delta t}{\Delta x} = 1$ and $v_{f,2}\frac{\Delta t}{\Delta x} < 1$.

Then we use the following Godunov finite difference equation for link $i = 1, \ldots, 8$ (Godunov, 1959):

$$\rho_{i,m}^{n+1} = \rho_{i,m}^{n} + \frac{\Delta t}{\Delta x}\left(q_{i,m-1/2}^{n} - q_{i,m+1/2}^{n}\right),$$

where $\rho_{i,m}^{n}$ is the average density in cell m of link i at time step n, and the boundary fluxes $q_{i,m-1/2}^{n}$ are determined by supply-demand methods. For upstream links $a = 1, \ldots, 4$, the in-fluxes are

$$q_{a,m-1/2}^{n} = \min\left\{D_{a,m-1}^{n}, S_{a,m}^{n}\right\}, \quad m = 1, \ldots, M_a,$$

where $D_{a,0}^{n}$ is the demand at origin a, and M_a is the number of cells on link a. For downstream links $b = 5, \ldots, 8$, the out-fluxes are

$$q_{b,m+1/2}^{n} = \min\left\{D_{b,m}^{n}, S_{b,m+1}^{n}\right\}, \quad m = 1, \ldots, M_b,$$

where $S_{b,M+1}^{n}$ is the supply at destination b, and M_b is the number of cells on link b. Then the in-fluxes of the downstream links and the out-flux of the upstream links are determined by the following intersection model (Jin and Zhang, 2004), which is the discrete version of the entropy condition in (20a) and (20c):

$$q^{n} = \min_{b=5}^{8}\left\{1, \frac{S_{b,1}^{n}}{\sum_{a=1}^{4} D_{a,M_a}^{n}\xi_{a\to b,M_a}^{n}}\right\}\sum_{a=1}^{4} D_{a,M_a}^{n},$$

$$q_{a\to b}^{n} = q^{n}\frac{D_{a,M_a}^{n}\xi_{a\to b,M_a}^{n}}{\sum_{a=1}^{2} D_{a,M_a}^{n}}, \quad a = 1, \ldots, 4; b = 5, \ldots, 8.$$

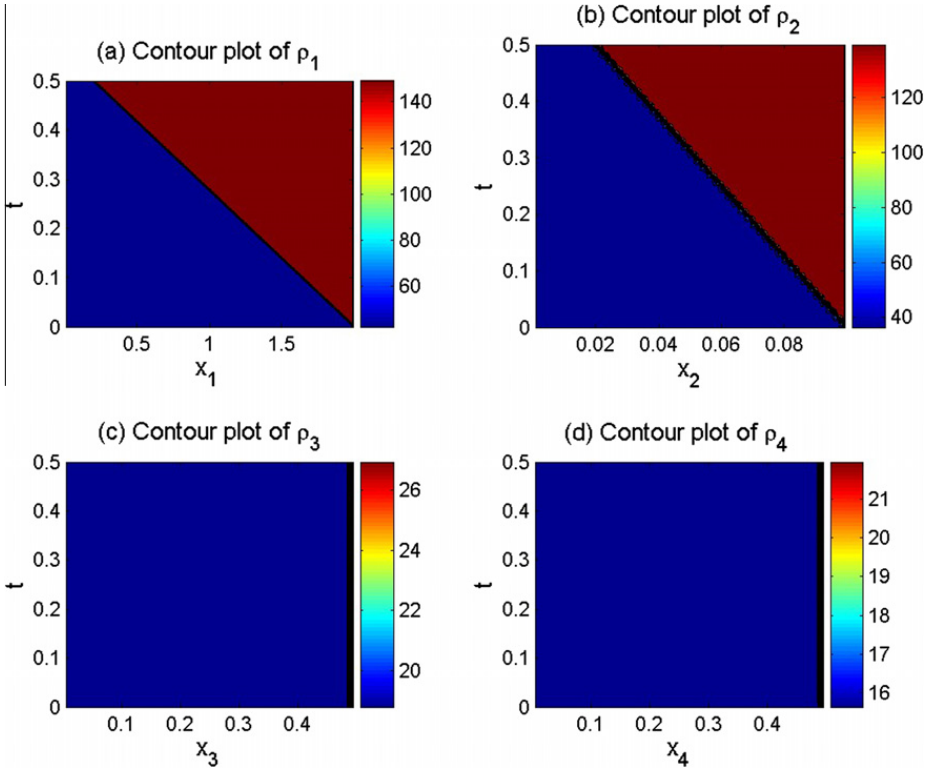

Fig. 9. Contour plots of traffic densities on upstream links.

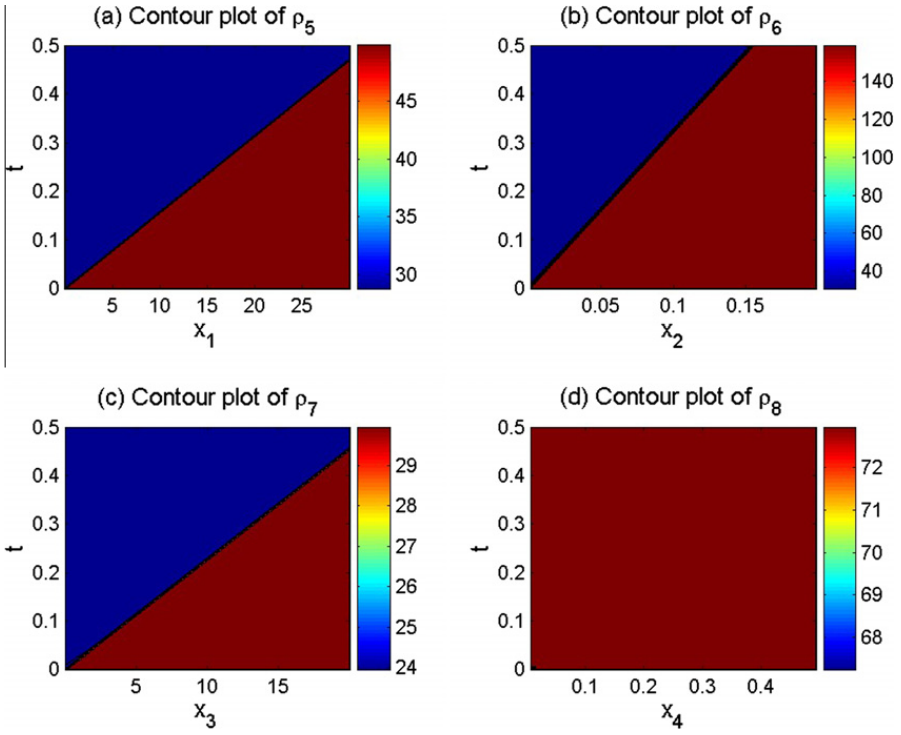

Fig. 10. Contour plots of traffic densities on downstream links.

We also track the commodity proportions in cell m on upstream links ($m = 1, \ldots, M_a$), $\xi^n_{a\to b,m}$, as follows (Jin and Zhang, 2004)

$$\xi^{n+1}_{a\to b,m} = \frac{\rho^n_{a,m}}{\rho^{n+1}_{a,m}}\xi^n_{a\to b,m} + \frac{\Delta t}{\Delta x}\frac{q^n_{a,m-1/2}\xi^n_{a\to b,m-1} - q_{a,m+1/2}\xi^n_{a\to b,m}}{\rho^{n+1}_{a,m}}.$$

In Fig. 9, we show the contour plots of traffic densities on upstream links 1, 2, 3, and 4; in Fig. 10, we show the contour plots of traffic densities on downstream links 5, 6, 7, and 8. Note that for links 2 and 6, we use smaller $\Delta x = 0.002$ km and $\Delta t = 0.000025$ h in order to have finer shock wave trajectories. From the figures, we can clearly see backward shock waves on links 1 and 2 and forward shock waves on links 5, 6, and 7. Stationary states will spread over these links after shock waves travel to the corresponding boundaries. On links 3 and 4, we can see interior states in the downstream cells next to the junction. These interior states only appear in one cell on each link, even if we shrink the cell size. The stationary states, interior states, shock wave speeds, and fluxes are all consistent with theoretical predictions in the preceding subsection.

6. Conclusion

In this paper, we first introduced a continuous multi-commodity kinematic wave model of a road network and defined its Riemann problem for a general junction with multiple upstream and downstream links. In supply-demand space we discussed two types of entropy conditions: one for feasible stationary and interior states, and the other based on fair merging and FIFO diverging rules for prescribing fluxes from interior states. After introducing the concept of critical demand level and separating upstream stationary states into strictly over-critical and under-critical states, we proved that solutions to the Riemann problem exist and are unique. Furthermore, with a simplified model of a four by four general intersection, we demonstrated that stationary states, interior states, and kinematic waves numerically solved from the multi-commodity Cell Transmission Model are consistent with those predicted by the theory.

With the new theory, we have the following observations for a general network junction: (i) When downstream supplies are sufficiently large, we have $\theta \geqslant 1$, and all upstream links become UC after a long time; i.e., all upstream queues dissipate in this case; (ii) When one or more downstream links do not have sufficient supplies, we have $l \geqslant 1$, some upstream links become congested (SOC), and some downstream links are starved (SUC); (iii) When upstream links become congested (SOC), their out-fluxes are proportional to their capacities, and it confirms that upstream vehicles merge in a fair manner. Therefore, the multi-commodity kinematic wave theory in (6) is physically meaningful, mathematically well-defined, and numerically consistent with the multi-commodity Cell Transmission Models with fair merging and FIFO diverging rules.

With entropy conditions given in (20), we find that interior states may be different from stationary states. The existence of interior states is also verified by the numerical example. However, interior states are inconsequential in determining kinematic waves on all links, and whether they exist in real traffic is subject to observations. From Theorem 4.7, we can introduce the following entropy condition to replace (20)

$$\theta = \max_{k=0}^{m} \min_{b=m+1}^{m+n} \frac{S_b^0 - \sum_{\alpha=k+1}^{m} D_\alpha^0 \xi_{\alpha\to b}^0}{\sum_{a=1}^{k} C_a \xi_{a\to b}^0}, \tag{41a}$$

$$D_1^0/C_1 \geqslant \cdots \geqslant D_l^0/C_l > \theta \geqslant D_{l+1}^0/C_{l+1} \geqslant \cdots \geqslant D_m^0/C_m, \tag{41b}$$

$$q = \sum_{a=1}^{l} \theta C_a + \sum_{\alpha=l+1}^{m} D_\alpha^0, \tag{41c}$$

$$q_a = \min\left\{D_a^0, \theta C_a\right\}, \tag{41d}$$

$$q_b = \sum_{a=1}^{l} q_a \xi_{a\to b}^0. \tag{41e}$$

The new entropy condition in (41) is equivalent to (20) except that interior states can always be the same as stationary states; i.e., we have the same fluxes if we replace interior states by stationary states in (41). If we implement (41) in CTM, then numerical boundary fluxes are always the same as theoretical ones, but it is not the case with (20). In other words, fluxes are invariant with (41), but not with (20) in numerical solutions. Even though (41) has nicer theoretical properties, the discrete version of (20) introduced in (Jin and Zhang, 2004) is much easier to be implemented in numerical solutions. Note that, even with invariant models as (41), it is still possible to have interior states different from stationary states in numerical solutions, as illustrated with the inhomogeneous LWR model (Jin and Zhang, 2003a; Jin et al., 2009). But in theoretical studies, it is simpler to avoid interior states by using the invariant Riemann solver.

From the discussions in this paper, we can see that a complete kinematic wave theory includes a system of hyperbolic conservation laws (6) and a proper junction model of merging and diverging rules. The first type of entropy conditions have to be satisfied by any kinematic wave models of network traffic flow (Holden and Risebro, 1995; Coclite et al., 2005). But one can have different types of merging and diverging rules for the second type of entropy conditions (e.g. Holden and Risebro, 1995; Coclite et al., 2005; Daganzo, 1995b; Lebacque and Khoshyaran, 2005; Jin and Zhang, 2004). In this sense, the multi-commodity kinematic wave theory is not complete for network traffic flow.[4] In (Holden and Risebro, 1995; Coclite et al., 2005), junction models have been presented in density-flux space. Here we can present a complete kinematic wave theory of network traffic flow in supply-demand space as follows. First, we have a commodity conservation law from (6):

$$\frac{\partial \xi_{p,a}(x_a,t)\rho_a(x_a,t)}{\partial t} + \frac{\partial \xi_{p,a}(x_a,t) q_a(x_a,t)}{\partial x_a} = 0. \tag{42a}$$

Second, the total boundary flux $q_a(x_a, t)$ is given by

$$q_a(x_a,t) = \min\left\{D_a\left(x_a^-,t\right), S_a\left(x_a^+,t\right)\right\}, \tag{42b}$$

where x_a^- and x_a^+ are the upstream and downstream points of x_a, respectively. Third, the commodity boundary flux $\xi_{p,a}(x_a, t)q_a(x_a, t)$ is given by

$$\xi_{p,a}(x_a,t) q_a(x_a,t) = \xi_{p,a}\left(x_a^-,t\right) \min\left\{D_a\left(x_a^-,t\right), S_a\left(x_a^+,t\right)\right\}, \tag{42c}$$

which is from the fact that commodity proportions always travel downstream. Finally, upstream demands, $D_a\left(x_a^-,t\right)$, and downstream supplies, $S_a\left(x_a^+,t\right)$, are determined by proper junction models: If x_a is inside a road link, the corresponding upstream demand and downstream supply can be easily determined by (8); If x_a is the downstream boundary of link a, which is at a general junction shown in (2), $D_a\left(x_a^-,t\right)$ is determined by (8), and the downstream supply is determined by

$$S_a(x_a^+,t) = \theta C_a, \tag{42d}$$

where θ is the critical demand level defined in Theorem 4.7; If x_a is the upstream boundary of link a, which is at another general junction, $S_a(x_a^+,t)$ is determined by (8), and the upstream demand is determined by

$$D_a(x_a^-,t) = \min_{\alpha=m+1,\alpha\neq a}^{m+n} \sum_{b=1}^{l} C_b \xi_{b\to a} \gamma_\alpha(l) + \sum_{-=l+1}^{m} D_\beta \xi_{\beta\to a}. \tag{42e}$$

In a sense, existing Cell Transmission Models can be considered as first-order numerical methods for solving the kinematic wave model, and it is possible to develop higher-order numerical methods within this framework (LeVeque, 2002). In this study, we only incorporated the fair merging and FIFO diverging rules into the entropy conditions. Other types of merging and diverging rules for three-legged junctions have been discussed in (Jin, 2010c; Jin, 2010b). If these rules can be extended

[4] Actually the LWR model for link traffic flow is not complete either. But for the LWR model, a unique Lax entropy condition is always implicitly assumed and consistent with the linear junction model (Ansorge, 1990; Lebacque, 1996).

to general junctions with multiple upstream and downstream links, they can be used to define entropy conditions in (20) and incorporated into the kinematic wave theory of general networks.

In Section 5, we only modeled merging and diverging conflicts among traffic streams at a general intersection. In (Chen et al., 2008), a more realistic discrete model of urban intersections was discussed. In reality, crossing conflicts among traffic streams could be more complicated, and more realistic intersection models can be incorporated into entropy conditions. For examples, we can add another constraint, $q \leqslant C_0$, to bound the intersection capacity, and integrate the macroscopic lane-changing model (Jin, 2010a). Traffic signals and stop signs at urban intersections could be incorporated into effective demands as in (Jin and Zhang, 2003b), and it is possible to analyze the effectiveness of fixed time, actuated, and other types of signal plans under different conditions with the theory. Also from the numerical example, we can see that total capacity is not fully utilized due to pre-defined route choices. Thus it is possible to maximize throughput with different signal plans. Similarly, the kinematic wave theory can be applied to evaluate and develop ramp metering schemes under simple conditions. For a road network with an upstream on-ramp and a downstream off-ramp, if the distance between the on-ramp and the off-ramp is very short, it is possible to simply consider it as a junction with two upstream links and two downstream links.

In this paper, we analyzed possible stationary states around a general junction with fair and FIFO diverging rules. Such stationary states can be considered as fixed points of the continuous kinematic wave model and the corresponding Cell Transmission Models. Another future research direction is to analyze possible stationary states in general road networks. Such a study would be helpful to understand such fundamental properties as capacities of a road network under stationary traffic. Then it is possible to analyze stationary capacity of a road network and drivers' route choice, departure time choice, and other network-level behaviors under stationary conditions. Such an analysis would be helpful for the design of road networks. Another possible application is to analyze impacts of earthquake or other events on performance of a road network.

References

Ansorge, R., 1990. What does the entropy condition mean in traffic flow theory? Transportation Research Part B 24 (2), 133–143.

Bar-Gera, H., Ahn, S., 2010. Empirical macroscopic evaluation of freeway merge-ratios. Transportation Research Part C 18 (4), 457–470.

Bliemer, M., 2007. Dynamic queuing and spillback in analytical multiclass dynamic network loading model. Transportation Research Record: Journal of the Transportation Research Board 2029, 14–21.

Braess, D., Nagurney, A., Wakolbinger, T., 2005. On a paradox of traffic planning. Transportation Science 39 (4), 446–450.

Buisson, C., Lebacque, J.P., Lesort, J.B., 1996. STRADA, a discretized macroscopic model of vehicular traffic flow in complex networks based on the Godunov scheme. In: CESA'96 IMACS Multiconference. Lille, France.

Bultelle, M., Grassin, M., Serre, D., 1998. Unstable Godunov discrete profiles for steady shock waves. SIAM Journal on Numerical Analysis 35 (6), 2272–2297.

Cassidy, M., Ahn, S., 2005. Driver turn-taking behavior in congested freeway merges. Transportation Research Record: Journal of the Transportation Research Board 1934, 140–147.

Chen, L., Jin, W., Hu, J., Zhang, Y., 2008. An urban intersection model based on multi-commodity kinematic wave theories. In: 11th International IEEE Conference on Intelligent Transportation Systems. pp. 269–274.

Coclite, G., Garavello, M., Piccoli, B., 2005. Traffic flow on a road network. SIAM Journal on Mathematical Analysis 36 (6), 1862–1886.

Courant, R., Friedrichs, K., Lewy, H., 1928. Über die partiellen Differenzengleichungen der mathematischen Physik. Mathematische Annalen 100, 32–74.

Dafermos, S.C., Sparrow, F.T., 1969. The traffic assignment problem for a general network. Journal of Research of the National Bureau of Standards: Part B 73 (2), 91–118.

Daganzo, C.F., 1995a. Properties of link travel time functions under dynamic loads. Transportation Research Part B 29 (2), 95–98.

Daganzo, C.F., 1995b. The cell transmission model II: network traffic. Transportation Research Part B 29 (2), 79–93.

Daganzo, C.F., 1996. The nature of freeway gridlock and how to prevent it. In: Proceedings of the 13th International Symposium on Transportation and Traffic Theory, pp. 629–646.

Daganzo, C.F., 1997. A continuum theory of traffic dynamics for freeways with special lanes. Transportation Research Part B 31 (2), 83–102.

Daganzo, C.F., 2002. A behavioral theory of multi-lane traffic flow. Part I: Long homogeneous freeway sections. II: Merges and the onset of congestion. Transportation Research Part B 36 (2), 131–169.

D'apice, C., Manzo, R., Piccoli, B., 2007. Packet flow on telecommunication networks. SIAM Journal on Mathematical Analysis 38 (3), 717–740.

D'Apice, C., Manzo, R., Piccoli, B., 2008. A fluid dynamic model for telecommunication networks with sources and destinations. SIAM Journal on Applied Mathematics 68 (4), 981–1003.

Del Castillo, J.M., Benitez, F.G., 1995. On the functional form of the speed–density relationship – II: Empirical investigation. Transportation Research Part B 29 (5), 391–406.

Durlin, T., Henn, V., 2008. Dynamic network loading model with explicit traffic wave tracking. Transportation Research Record: Journal of the Transportation Research Board 2085, 1–11.

Engquist, B., Osher, S., 1980. Stable and entropy satisfying approximations for transonic flow calculations. Mathematics of Computation 34 (149), 45–75.

Formaggia, L., Lamponi, D., Quarteroni, A., 2003. One-dimensional models for blood flow in arteries. Journal of Engineering Mathematics 47 (3), 251–276.

Garavello, M., Piccoli, B., 2005. Source–destination flow on a road network. Communications in Mathematical Sciences 3 (3), 261–283.

Garavello, M., Piccoli, B., 2006a. Traffic flow on a road network using the Aw-Rascle model. Communications in Partial Differential Equations 31 (2), 243–275.

Garavello, M., Piccoli, B., 2006b. Traffic Flow on Networks, vol. 1. Applied Mathematics Series.

Gazis, D.C., Herman, R., Rothery, R.W., 1961. Nonlinear follow-the-leader models of traffic flow. Operations Research 9 (4), 545–567.

Gipps, P.G., 1986. A model for the structure of lane changing decisions. Transportation Research Part B 20 (5), 403–414.

Godunov, S.K., 1959. A difference method for numerical calculations of discontinuous solutions of the equations of hydrodynamics. Matematicheskii Sbornik 47 (3), 271–306 (in Russia).

Gottlich, S., Herty, M., Klar, A., 2005. Network models for supply chains. Communications in Mathematical Sciences 3 (4), 545–559.

Greenshields, B.D., 1935. A study in highway capacity. Highway Research Board Proceedings 14, 448–477.

Haut, B., Bastin, G., 2007. A second order model of road junctions in fluid models of traffic networks. Networks and Heterogeneous Media 2 (2), 227.

Herty, M., Kirchner, C., Moutari, S., Rascle, M., 2008. Multicommodity flows on road networks. Communications in Mathematical Sciences 6 (1), 171–187.

Herty, M., Klar, A., 2003. Modeling, simulation, and optimization of traffic flow networks. SIAM Journal on Scientific Computing 25 (3), 1066–1087.

Herty, M., Moutari, S., Rascle, M., 2006. Optimization criteria for modelling intersections of vehicular traffic flow. Networks and Heterogeneous Media 1 (2), 275–294.

Hidas, P., 2002. Modelling lane changing and merging in microscopic traffic simulation. Transportation Research Part C 10 (5–6), 351–371.

Hidas, P., 2005. Modelling vehicle interactions in microscopic simulation of merging and weaving. Transportation Research Part C 13 (1), 37–62.
Holden, H., Risebro, N.H., 1995. A mathematical model of traffic flow on a network of unidirectional roads. SIAM Journal on Mathematical Analysis 26 (4), 999–1017.
Jin, W.-L., 2009. Asymptotic traffic dynamics arising in diverge-merge networks with two intermediate links. Transportation Research Part B 43 (5), 575–595.
Jin, W.-L., 2010a. A kinematic wave theory of lane-changing traffic flow. Transportation Research Part B 44 (8-9), 1001–1021.
Jin, W.-L., 2010b. Analysis of Kinematic Waves Arising in Diverging Traffic Flow Models. Arxiv preprint. <http://arxiv.org/abs/1009.4950>.
Jin, W.-L., 2010c. Continuous kinematic wave models of merging traffic flow. Transportation Research Part B 44 (8-9), 1084–1103.
Jin, W.-L., Chen, L., Puckett, E.G., 2009. Supply-demand diagrams and a new framework for analyzing the inhomogeneous Lighthill–Whitham–Richards model. In: Proceedings of the 18th International Symposium on Transportation and Traffic Theory, pp. 603–635.
Jin, W.-L., Zhang, H.M., 2003a. The inhomogeneous kinematic wave traffic flow model as a resonant nonlinear system. Transportation Science 37 (3), 294–311.
Jin, W.-L., Zhang, H.M., 2003b. On the distribution schemes for determining flows through a merge. Transportation Research Part B 37 (6), 521–540.
Jin, W.-L., Zhang, H.M., 2004. A multicommodity kinematic wave simulation model of network traffic flow. Transportation Research Record: Journal of the Transportation Research Board 1883, 59–67.
Lax, P.D., 1972. Hyperbolic Systems of Conservation Laws and the Mathematical Theory of Shock Waves. SIAM, Philadelphia, Pennsylvania.
Lebacque, J.P., 1996. The Godunov scheme and what it means for first order traffic flow models. In: Proceedings of the 13th International Symposium on Transportation and Traffic Theory, pp. 647–678.
Lebacque, J.P., 2005. Intersection modeling, application to macroscopic network traffic flow models and traffic management. In: Hoogendorn, S., Luding, S., Bovy, P., Schreckenberg, M., Wolf, D. (Eds.), Traffic and Granular Flow '03. Springer, pp. 261–278.
Lebacque, J.P., Khoshyaran, M., 2005. First order macroscopic traffic flow models: intersection modeling, network modeling. In: Proceedings of the 16th International Symposium on Transportation and Traffic Theory, pp. 365–386.
LeVeque, R.J., 2002. Finite Volume Methods for Hyperbolic Problems. Cambridge University Press, Cambridge; New York.
Lighthill, M.J., Whitham, G.B., 1955. On kinematic waves: II. A theory of traffic flow on long crowded roads. Proceedings of the Royal Society of London A 229 (1178), 317–345.
Liu, G., Lyrintzis, A.S., Michalopoulos, P.G., 1996. Modelling of freeway merging and diverging flow dynamics. Applied Mathematical Modelling 20 (6), 459–469.
Lo, H., Szeto, W., 2002. A cell-based variational inequality formulation of the dynamic user optimal assignment problem. Transportation Research Part B 36 (5), 421–443.
Merchant, D., Nemhauser, G., 1978. A model and an algorithm for the dynamic traffic assignment problems. Transportation Science 12 (3), 183–199.
Muñoz, J.C., Daganzo, C.F., 2002. The bottleneck mechanism of a freeway diverge. Transportation Research Part A 36 (6), 483–505.
Newell, G., 1980. Traffic Flow on Transportation Networks. MIT Press, MA.
Ni, D., Leonard, J., 2005. A simplified kinematic wave model at a merge bottleneck. Applied Mathematical Modelling 29 (11), 1054–1072.
Papageorgiou, M., 1990. Dynamic modelling, assignment and route guidance in traffic networks. Transportation Research Part B 24 (6), 471–495.
Papageorgiou, M., Kotsialos, A., 2002. Freeway ramp metering: an overview. IEEE Transactions on Intelligent Transportation Systems 3 (4), 271–281.
Payne, H.J., 1971. Models of freeway traffic and control. In: Mathematical Models of Public Systems. Simulation Councils Proceeding Series, vol. 1. pp. 51–60.
Richards, P.I., 1956. Shock waves on the highway. Operations Research 4 (1), 42–51.
Ruan, W., Clark, M., Zhao, M., Curcio, A., 2003. A hyperbolic system of equations of blood flow in an arterial network. SIAM Journal on Applied Mathematics 64 (2), 637–667.
Sheffi, Y., Mahmassani, H., Powell, W., 1982. A transportation network evacuation model. Transportation Research Part A 16 (3), 209–218.
Sherwin, S., Franke, V., Peiró, J., Parker, K., 2003. One-dimensional modelling of a vascular network in space–time variables. Journal of Engineering Mathematics 47 (3), 217–250.
van Leer, B., 1984. On the relation between the upwind-differencing schemes of Godunov, Engquist–Osher and Roe. SIAM Journal on Scientific and Statistical Computing 5 (1), 1–20.
Wardrop, J.G., 1952. Some theoretical aspects of road traffic research. In: Proceedings of the Institute of Civil Engineers, Part II 1, pp. 325–378.
Whitham, G.B., 1974. Linear and Nonlinear Waves. John Wiley and Sons, New York.
Wu, J., Chen, Y., Florian, M., 1998. The continuous dynamic network loading problem: a mathematical formulation and solution method. Transportation Research Part B 32 (3), 173–187.
Zhang, H.M., Jin, W.-L., 2002. Kinematic wave traffic flow model for mixed traffic. Transportation Research Record: Journal of the Transportation Research Board 1802, 197–204.